Progress in Oceanography 137 (2015) 314–333

Contents lists available at ScienceDirect

Progress in Oceanography

journal homepage: www.elsevier.com/locate/pocean

Review

Kuroshio intrusion into the South China Sea: A review

Feng Nan [a], Huijie Xue [b,c], Fei Yu [a,*]

[a] Key Laboratory of Ocean Circulation and Wave Studies, Institute of Oceanology, Chinese Academy of Sciences, Qingdao, China
[b] State Key Laboratory of Tropical Oceanography, South China Sea Institute of Oceanology, Chinese Academy of Sciences, Guangzhou, China
[c] School of Marine Sciences, University of Maine, Orono, ME, USA

ARTICLE INFO

Article history:
Received 1 August 2013
Received in revised form 15 May 2014
Accepted 26 May 2014
Available online 14 June 2014

ABSTRACT

The Kuroshio carrying the northwestern Pacific water intrudes into the South China Sea (SCS) through the Luzon Strait, significantly affecting the temperature, salinity, circulation, and eddy generation in the SCS. Thus, the Kuroshio intrusion makes important contributions to the momentum, heat and salt budgets in the SCS. In the past decades, much work has been done on the Kuroshio intrusion. This paper reviews past efforts and summarizes our current understanding of the Kuroshio intruding processes from observational evidence, laboratory results, theoretical analyses, and a range of numerical model simulations. In addition, discrepancies between results simulated by models, as well as those between simulations and observations, are presented. Specifically, this paper addresses the following topics: (1) different types of the Kuroshio intrusion into the SCS and their identification, (2) vertical structure of the Kuroshio in the Luzon Strait, (3) an overview of the Luzon Strait transport resulting from observations and numerical model simulations, (4) seasonal and interannual variations of the Kuroshio intrusion, as well as eddy generation due to the Kuroshio path variation, and (5) dynamical mechanisms (*e.g.*, wind forcing, interbasin pressure gradient, β effect and hysteresis, potential vorticity, eddy activity) controlling the Kuroshio intrusion into the SCS. Finally, several future research topics for gaining a better understanding of the Kuroshio intruding processes are suggested.

Contents

* Corresponding author. Address: Institute of Oceanology, Chinese Academy of Sciences, 7 Nanhai Road, Qingdao 266071, China. Tel.: +86 053282898187; fax: +86 053282898186.
E-mail address: yuf@qdio.ac.cn (F. Yu).

http://dx.doi.org/10.1016/j.pocean.2014.05.012
0079-6611/

Introduction

The Kuroshio originates from the North Equatorial Current (NEC). The NEC in the North Pacific Ocean is located between the subtropical and tropical gyres (Fig. 1), playing an important role in mass and heat transport to the western Pacific warm pool and global thermohaline circulation via the Indonesian Throughflow. After encountering the western boundary, the NEC bifurcates into the southward-flowing Mindanao Current (MC) and the northward-flowing Kuroshio near the Philippine coast (*e.g.*, Nitani, 1972; Qiu and Lukas, 1996; Qu and Lukas, 2003; Zhai and Hu, 2013). This partition of the water mass as well as the heat transport between the poleward and equatorward flows, not only has a great influence upon the low-latitude Western Boundary Current (WBC), but is also believed to be important in determining the interactions between the atmosphere and ocean (Qiu and Lukas, 1996). The NEC, the MC, and the Kuroshio comprise the NMK current system as shown in Fig. 1. Mass and heat exchange between the tropical and subtropical gyres in the North Pacific can occur due to the fluctuations in the NMK system (Qu and Lukas, 2003). The NMK system exhibits strong seasonal and interannual variabilities since they are in a geographical location where dynamic processes are dominated by the monsoons and El Niño-Southern Oscillation (ENSO) (Kim et al., 2004).

The Kuroshio carrying the northwestern Pacific water flows northward along the east Philippine coast. When passing by the Luzon Strait, a branch of the Kuroshio flows northwestward into the South China Sea (SCS) mainly through the Balintang Channel (*e.g.*, Chern and Wang, 1998; Liang et al., 2003, 2008; Yuan et al., 2008a). Most of the Kuroshio water flows out of the SCS subsequently through the Bashi Channel, but some water intrudes into the SCS (Fig. 2). The latter affects the temperature, salinity, circulation, eddy generation in the northeastern SCS, making important contributions to the momentum, heat and salt budgets in the SCS (*e.g.*, Li et al. 1998; Xu and Su 2000; Qu et al., 2004; Wu and Chiang 2007; Xiu et al. 2010; Nan et al., 2011b; Wu, 2013).

The Kuroshio intrusion into the SCS has gained increasing attention over the past few decades. Although some characteristics have been illustrated, the Kuroshio intruding processes and its controlling mechanisms are still not well understood. Similar to the northwestern Pacific water, the T–S curve of the SCS water appears as an approximately mirrored 'S', providing evidence of the northwestern Pacific water in the SCS (Shaw, 1991; Qu et al., 2000). The Kuroshio intrusion has a seasonal pattern with the intrusion being stronger in winter than in summer (Wyrtki, 1961; Shaw, 1991). The surface Kuroshio water can intrude deep into the SCS especially in winter (Centurioni et al., 2004). Compared with seasonal variability, less is known about the interannual variability of the Kuroshio intrusion due to limited available observations (Wu, 2013). In the Luzon Strait, eastward and westward flows often appear alternately (*e.g.*, Nitani, 1972; Xu et al., 2004; Zhou et al., 2009). The reason is still unknown. Estimates of the Luzon Strait transport (LST) vary from a few Sv to more than ten Sv (*e.g.*, Xu and Su, 2000; Qu et al., 2006; Tian et al., 2006; Yuan et al., 2008b). On an interannual time scale, the LST from the Pacific into the SCS tends to be higher/lower during El Niño/La Niña years, and seems to be a key process conveying the climate signal from the Pacific into the SCS (Qu et al., 2004; Liu et al., 2008). Results from observation (Caruso et al., 2006), numerical models (Sheremet, 2001; Xue et al., 2004; Wu and Chiang, 2007; Sheu et al., 2010), and laboratory experiments (Sheremet and Kuehl, 2007; Kuehl and Sheremet, 2009) all showed that the Kuroshio takes different intruding paths southwest of Taiwan. Kuroshio intruding path can change from one path to another in several weeks (Nan et al., 2011a). Changes of the Kuroshio path often induce eddies (Nan et al., 2011c). Eddy generation exhibits strong seasonal and interannual variabilities due to changes of the Kuroshio intruding path. The mechanism leading to the Kuroshio intrusion and the LST remains controversial to date. Wind forcing (*e.g.*, Wang and Chern, 1987; Farris and Wimbush, 1996; Metzger and Hurlburt, 2001a; Wang et al., 2006c; Kuehl and Sheremet, 2009; Wu and Hsin, 2012), interbasin pressure gradient (*e.g.*, Metzger and

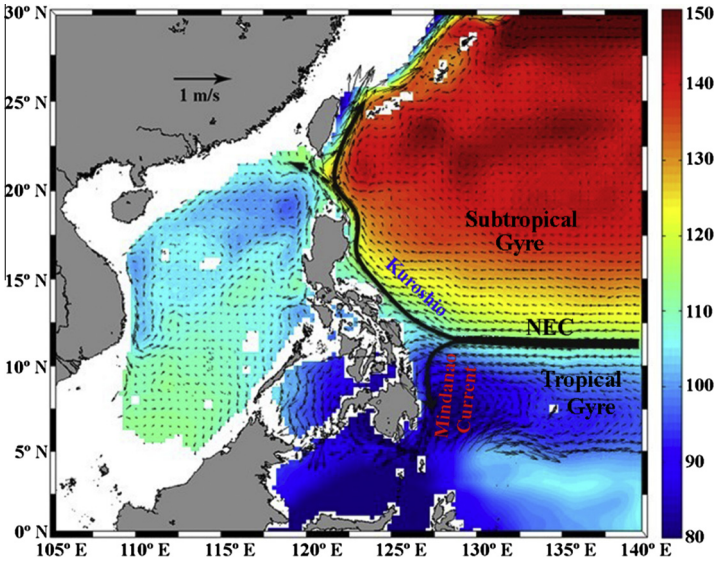

Fig. 1. Mean Absolute Dynamic Topography (ADT) (units: cm) and the corresponding surface geostrophic currents (units: m s^{-1}) derived from the 18-year (1993–2010) satellite altimeter data. Black solid lines represent a schematic of the NMK current system.

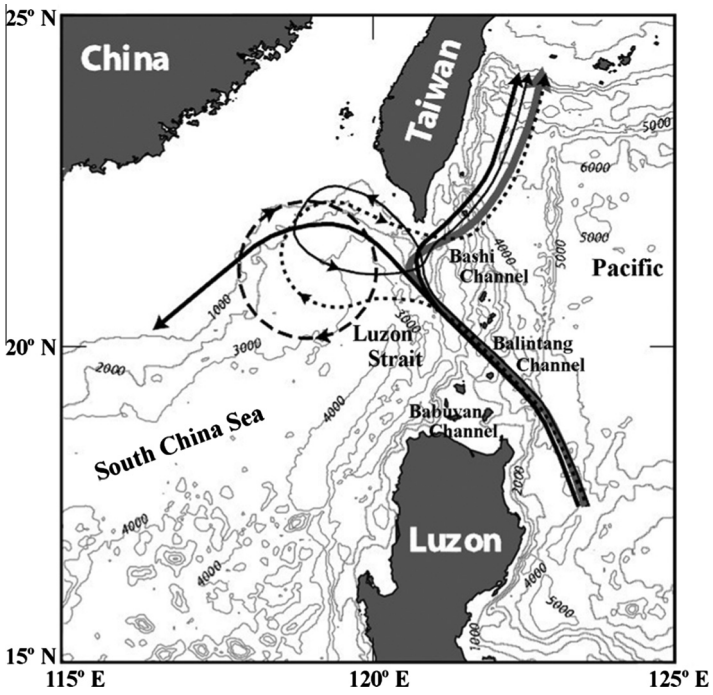

Fig. 2. Topography in the vicinity of the LS and the sketch of the different types of Kuroshio intrusions (adapted from Caruso et al., 2006). Isobath depths are in meters.

Hurlburt, 1996; Qu, 2000; Song, 2006), β effect and hysteresis (*e.g.,* Sheremet, 2001; Yuan, 2002; Sheremet and Kuehl, 2007; Yuan and Wang, 2011), potential vorticity (PV) (*e.g.,* Sheu et al., 2010; Xue et al., 2004), and eddy activity (*e.g.,*Liu et al., 2005; Nan et al., 2011c; Yang et al., 2013a; Lu and Liu, 2013) may potentially contribute to the Kuroshio intruding processes, indicating that the complexity of the Kuroshio intrusion.

In the past decades, much work has been done on the Kuroshio intrusion into the SCS through the Luzon Strait. Several dozen papers have been published, and much of what is known about the characteristics of the Kuroshio intrusion comes from these extensive and comprehensive studies (*e.g.,* Dale, 1956; Wyrtki, 1961; Nitani, 1972; Shaw, 1991; Farris and Wimbush, 1996; Liang et al., 2008). Hu et al. (2000) and Liu et al. (2008) reviewed the advances in ocean circulation research in the SCS that includes the Kuroshio intrusion. However, they did not elaborate sufficiently on the Kuroshio patterns in the Luzon Strait, its seasonal and interannual variations, and dynamical mechanisms. This paper is broader in scope and focuses on the latest advances. We review past efforts and summarize our current understanding of the Kuroshio intruding processes from observational evidence, laboratory results, theoretical analyses, and a range of numerical model simulations. We begin in this section with an overview of the origin of the Kuroshio and the upper ocean circulations in the northwestern Pacific that provide the background state. The rest of the paper is organized as follows. Section 'Paths of the Kuroshio intrusion into the SCS' examines different types of the Kuroshio intrusion into the SCS and their identification. Section 'Vertical structure of the Kuroshio in the Luzon Strait' presents the vertical structure of the Kuroshio in the Luzon Strait. Se ction 'Transport of the Kuroshio intrusion into the SCS' provides an overview of the LST resulting from observations and numerical model simulations. Section 'Seasonal and interannual variations of the Kuroshio intrusion into the SCS' focuses on seasonal and interannual variations of the Kuroshio intrusion into the SCS, as well as eddy generation due to the Kuroshio path variation. Secti on 'Dynamical mechanisms' discusses the possible mechanisms contributing to the Kuroshio intruding processes. Finally, Section 'Summary and future research' summarizes the main research findings over the past few decades and highlights topics that merit further investigation.

Paths of the Kuroshio intrusion into the SCS

It was a debated issue on how the Kuroshio intrudes into the SCS in history. Hu et al. (2000) reviewed some views before 2000, in which several different stable paths of the Kuroshio intrusion were proposed due to the lack of long-term consecutive observations (*e.g.*, Dale, 1956; Qiu et al., 1984; Li and Wu, 1989; Li et al., 1998). *In situ* 138 measurements in the research area, though limited, have provided quite valuable information and have laid the foundation for 139 our present understanding of the Kuroshio 140 intrusion. Existence of different types of the Kuroshio intruding path have been verified by model simulations (Metzger and Hurlburt, 2001a; Sheremet, 2001; Xue et al., 2004), laboratory experiments (Sheremet and Kuehl, 2007; Kuehl and Sheremet, 2009), and consecutive satellite observations (Yuan et al., 2006; Caruso et al., 2006). An important understanding change after 2000 is that the Kuroshio intruding path may be unstable. In this section, we summarize those typical views in history and focus on the results after 2000.

Different types of the Kuroshio intrusion into the SCS

According to Hu et al. (2000), there had been four different views on how the Kuroshio intrudes into the SCS and they were "Kuroshio direct branch", "Kuroshio Current Loop (KCL)", "Kuroshio extension", and "Anticyclonic rings". It was noted that there existed a branch of the Kuroshio intrusion into the SCS by early researches (Dale, 1956; Nitani, 1972). The Kuroshio branch was observed by Qiu et al. (1984) based on the float measured currents and historical observations in the northern SCS and named as the SCS Branch of Kuroshio (SCSBK). However, no obvious intruding branch was observed in some years (*e.g.*, Li et al., 2002; Xu et al., 2007; Chen et al., 2010). The view of KCL was proposed by Li and Wu (1989). They suggested that there is a KCL southwest of Taiwan and the loop can extend to 116°–117°E. The KCL was

reproduced in several models (*e.g.,* Farris and Wimbush, 1996; Chern and Wang, 1998; Sheremet, 2001; Jia and Liu, 2004; Xue et al., 2004; Wu and Chiang, 2007; Chern et al., 2010; Sheu et al., 2010). An anticyclonic warm core eddy shedding from the KCL was reported by Li et al. (1998). The characteristics of the shedding eddy and its propagation were investigated using 17-year satellite altimeter data by Nan et al. (2011c). The detailed description for the four views can be seen from Hu et al. (2000), which will not be repeated here. In short, different researchers proposed different views on how the Kuroshio intrudes into the SCS based on limited historical observations or numerical models.

It can be inspected that the Kuroshio may take different intruding paths southwest of Taiwan, i.e., the Kuroshio intruding path is unstable. At the beginning of this century, Metzger and Hurlburt (2001a) pointed out that Kuroshio penetration and eddy shedding are nondeterministic on annual and interannual timescales caused by mesoscale flow instabilities in the Luzon Strait. Using a single layer depth-averaged approach, Sheremet (2001) formulated an idealized model of a western boundary current encountering a gap in the western wall. Multiple flow patterns (leaping the gap or penetrating the gap) exist in such system, which was confirmed by their subsequent laboratory experiments of the gap-leaping WBC (Sheremet and Kuehl, 2007; Kuehl and Sheremet, 2009). The model of Xue et al. (2004) depicted both the KCL and the SCSBK depending on the current speed and intruding angle. Increasing remote sensing images provide conclusive evidence for the change process of the Kuroshio intrusion. For instance, Yuan et al. (2006) analyzed satellite ocean color, SST, and altimeter data and demonstrated that the KCL is a transient phenomenon rather than a persistent circulation pattern. Caruso et al. (2006) depicted five different types of Kuroshio intrusion into the SCS based on satellite data, including a small anticyclonic bend in the Luzon Strait, the SCSBK, the KCL, a detached anticyclonic eddy, and a cyclonic loop northwest of the Luzon Strait (Fig. 2). Their work describes almost all types of the Kuroshio intruding paths and eddy-current structure southwest of Taiwan. Identification of different types of the Kuroshio intrusion into the SCS will be discussed in the ensuing section.

Identification of three types of the Kuroshio intrusion into the SCS

Although multiple flow patterns for the Kuroshio intrusion have been descriptive and schematic, how to define an index to distinguish different types of Kuroshio intrusion quantitatively is significantly important to understand the Kuroshio intruding processes and dynamics. The index should be derived based on readily available observations (*e.g.,* satellite remote sensing data) or credible ocean model output. Furthermore, the definition should be simple to use and can be applied to multiple data sets consistently. There have been several different indices proposed each with its own advantages and disadvantages.

The maximum and minimum salinity of the subsurface and intermediate waters are good tracers to delineate the Kuroshio and SCS waters since the maximum (minimum) salinity of the Kuroshio water is notably higher (lower) than those of the SCS water (*e.g.*, Li et al., 2002; Qu et al., 2000; Zhou et al., 2009; Chen et al., 2010). Yu et al. (2013) proposed an improved method of quantifying the penetration of the Kuroshio into the Luzon Strait based on simulated salinity from 1971 to 2006 of high-resolution ROMS model. An index was defined that represents a composite average of the standardized salinity in the region southwest of Taiwan bounded by 0.6 correlation coefficient contour between salinity series at the 20°N, 118°E and other points. This index can be used for indicating variation of the Kuroshio intruding strength and can also be applied to the subsurface layer using simulated subsurface salinity. However, the historical observations of the salinity in the Luzon Strait region are very rare. Modeled salinity is often far from the observational value (Nan et al., 2011a, 2013). That is why there are few results on the Kuroshio intrusion based on modeled salinity in our study area. Thus one cannot establish a long-term index based on the salinity to quantify the Kuroshio intruding strength of different paths.

Long-term and high-resolution sea surface information from satellite is readily available. The Kuroshio temperature is higher than that of the SCS water. It seems that the two waters can be distinguished according to temperature difference. However, as the SCS water warms significantly in summer, which decreases the temperature difference between the Kuroshio and the SCS surface water, making it difficult to distinguish the two waters (Farris and Wimbush, 1996). SST is thus not a good indicator to distinguish the Kuroshio water from the SCS water. Su et al. (2010) developed an objective classification method to distinguish the water masses of Kuroshio and SCS by using an artificial neural network model. This method was verified by comparison with analysis of water masses based on *in situ* data in 2006. However, it is unclear whether it could be used to detect spatial and temporal distributions the Kuroshio intusion since satellite remote sensing of SST and ocean-color is often limited by cloud cover (see Fig. 3 in Su et al., 2010). Mean SSH in the western Pacific is higher than that of the SCS (Fig. 1). Conceptually, the Kuroshio intrusion can carry higher SSH into the SCS. According to Nan et al. (2011a), it is also difficult to identify the Kurishio water and the SCS water based on the SSH difference quantitatively. Thus neither SST nor SSH is a good indicators to quantatively distinguish the Kuroshio water from the SCS water.

The combination of several satellites (Jason-1&2, Topex/Poseidon, Envisat, GFO, ERS, and Geosat) enables consecutive (weekly from October 1992 to now) and high-precision (1/4°) altimetry data. Although both tidal and sea level pressure corrections are incorporated, the satellite data in shelf areas could still be contaminated by aliases from tides and internal waves. So the data in areas where the water depth is less than 200 m are often excluded (Yuan et al., 2006; Nan et al., 2011a, 2011b). Based on previous studies and analysis of the geostrophic velocity derived from the weekly satellite SSH maps, Nan et al. (2011a) suggested that the KCL, the SCSBK, and the Kuroshio leaping across the Luzon Strait are three main patterns for the Kuroshio intrusion into the SCS. They were named as the looping path, the leaking path, and the leaping path, respectively (i.e., 3L model). A Kuroshio SCS Index (KSI) is defined by Nan et al. (2011a) using the integral of geostrophic vorticity southwest of Taiwan (118°E–121°E, 19°N–23°N) as the following,

$$KSI = \int\int (-(g/f)\nabla^2\eta)dA \quad (1)$$

to distinguish the three types. Here η is SSH; g is the gravity acceleration; and f is the Coriolis parameter. Stronger anticyclonic currents correspond to larger negative KSI, while stronger cyclonic currents correspond to larger positive KSI. Three typical paths can be easily identified based on the KSI derived from the weekly satellite ADT from 1993 to 2008 (see Fig. 3 in Nan et al., 2011a).

The index proposed by Nan et al. (2011a) is simple to use and can also be applied to ocean model output. Using this index, identification of the looping path is robust based on analysis of the geostrophic velocity derived from the weekly satellite altimeter data. However, identification of the leaping path is not as robust because around the stronger cyclonic currents there is often anticyclonic eddy generated (Nan et al., 2011c). Nan (2012) modified the index to identify the three Kuroshio paths. The KSI was again used to identify the looping path. However, when the Kuroshio leaps across the Luzon Strait, the transport through the Luzon Strait is eastward or the water flows from the SCS to the Pacific.

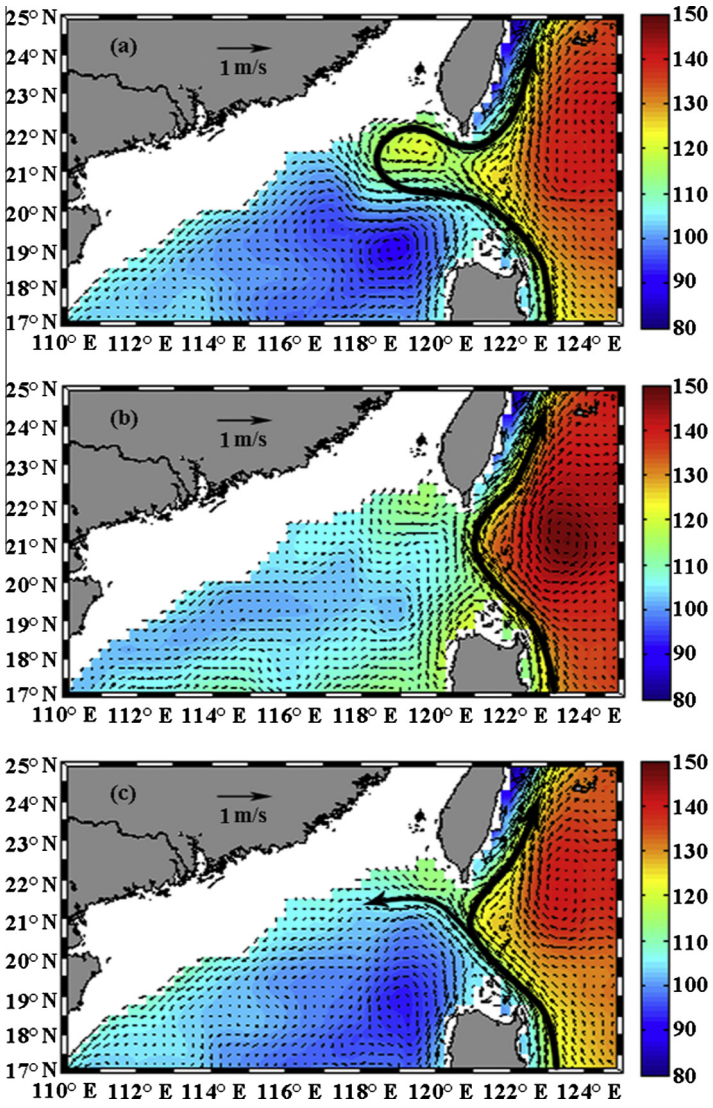

Fig. 3. The mean ADT (unit: centimeters) and the corresponding surface geostrophic currents associated with the three types of Kuroshio intrusion: the looping path (a), the leaping path (b), and the leaking path (c). Black line represents the Kuroshio axis. Adapted from Nan et al. (2011a).

Hence the surface LST (per unit depth) was calculated to identify the leaping path. When the surface LST is eastward, the leaping path occurs. It should be noted that the surface LST may also be eastward when the looping path occurs. So when identifying the three types, the looping path should be identified firstly based on the KSI index. Then the surface LST index is used to identify the leaping path. After the looping path and the leaping path are identified, the leaking path is left. Using the method above, the three typical paths for the Kuroshio intrusion can be distinguished based on long-time series satellite data or model outputs (Nan, 2012). It is noteworthy that the above method for identification of the Kuroshio paths is limited by the uncertainty of the SSH, the derived geostrophic currents and geostrophic vorticity, the region of KSI box, section for calculating the LST. Fig. 3 shows the mean SSH and the corresponding surface geostrophic currents associated with the three types of Kuroshio intrusion: the looping path, the leaking path, and the leaping path. Subsurface salinity maximum and intermediate salinity minimum distributions associated with the looping path, the leaking path, and the leaping path can be seen from Fig. 9 in Nan et al. (2011a).

Identification of three types of the Kuroshio intrusion quantitatively is significantly important to understand the Kuroshio intruding processes and its seasonal and interannual variations (see Section 'Seasonal and interannual variations of the Kuroshio intrusion into the SCS'). According to Nan, 2012, the leaking path is the most frequent form with the probability of occurrence at 44.8%, while the probability of occurrence for the leaping path is 39.5%. The probability of occurrence for the looping path is 15.7%, indicated that the KCL is not a persistent circulation pattern in the Luzon Strait area which is consistent with the result of Yuan et al. (2006). It can be speculated that different forms of the Kuroshio intrusion correspond to different mechanisms. Clarifying the dynamics of each intruding form is crucial for understanding the mechanism of the Kuroshio intusion. Note that the Kuroshio path in the Luzon Strait can change from one path to another in several weeks, which is the main reason that eddies often form southwest of Taiwan. Eddies generation due to the change of the Kuroshio path will be discussed in Section 'Eddy generation due to change of the Kuroshio paths'.

Vertical structure of the Kuroshio in the Luzon Strait

Luzon Strait is the main conduit for water exchange between the SCS and the western Pacific. It is about 360 km in width and

consists of three narrow passages (Bashi Channel, Balintang Channel, and Babuyan Channel) separated by many small islands in the strait (Fig. 2). Due to complex bathymetry and instability of the Kuroshio, the vertical structure of the current in the Luzon Strait is complex too. Snapshot measurements showed that both eastward and westward currents alternate spatially across the Luzon Strait. Wyrtki (1961) noted that the flow in Luzon Strait changes its sign at about 300 m in winter and at about 400 m in summer. Nitani (1972) analyzed the hydrographic data and pointed out that in the 120°10′E section across the Luzon Strait, the eastward and westward flows appeared alternately, and the current speed changed from year to year. Xu et al. (2004) and Zhou et al. (2009) also observed that the eastward and westward flows appeared alternately at the 120°E section. It should be noted that the current pattern is different along different meridional sections in the Luzon Strait (Chen et al., 2011b). Fig. 4 shows the geostrophic flows at 120°E, 120.5°E, and 121°E based on CTD data. It can be seen that the position and speed of eastward and westward flows are significantly different. The SCS outflows at 18.5°–19.2°N at 120°E (Fig. 4a) are much stronger than that at 121°E (Fig. 4c). Therefore, the snapshot measurements of alternating currents and the LST at 120°E may not be representative of the water exchange between the SCS and the Pacific at all times.

In order to capture the Kuroshio axis, we set the observational section at 120.75°E where Luzon Strait is narrowest (see also Hsin et al., 2012). Fig. 5 shows the annual mean temperature, salinity, and zonal velocity at 120.75°E from 2004 to 2012 based on the HYCOM output. The horizontal resolution of the global daily outputs is 1/12°. It assimilates available satellite altimeter observations and *in situ* vertical temperature and salinity profiles. The model results have been validated against the observations (see

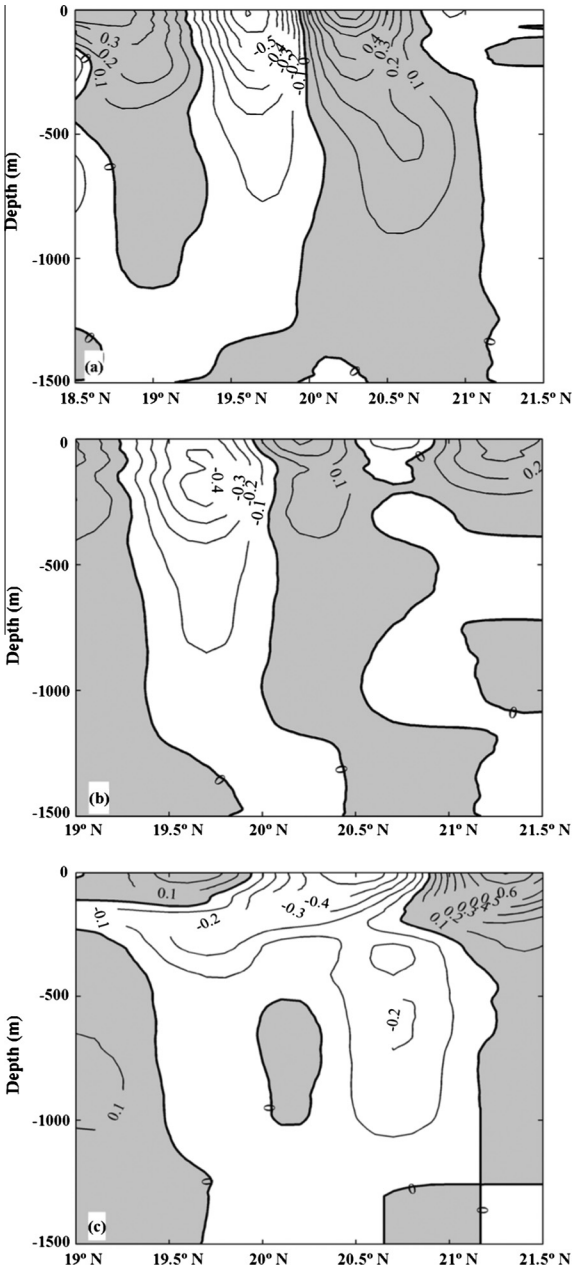

Fig. 4. Geostrophic flows at 120°E (a), 120.5°E (b), and 121°E (c) in the Luzon Strait based on CTD data from June 21 to July 5 in 2009. Positive (negative) values represent eastward (westward) currents (from Chen et al., 2011b).

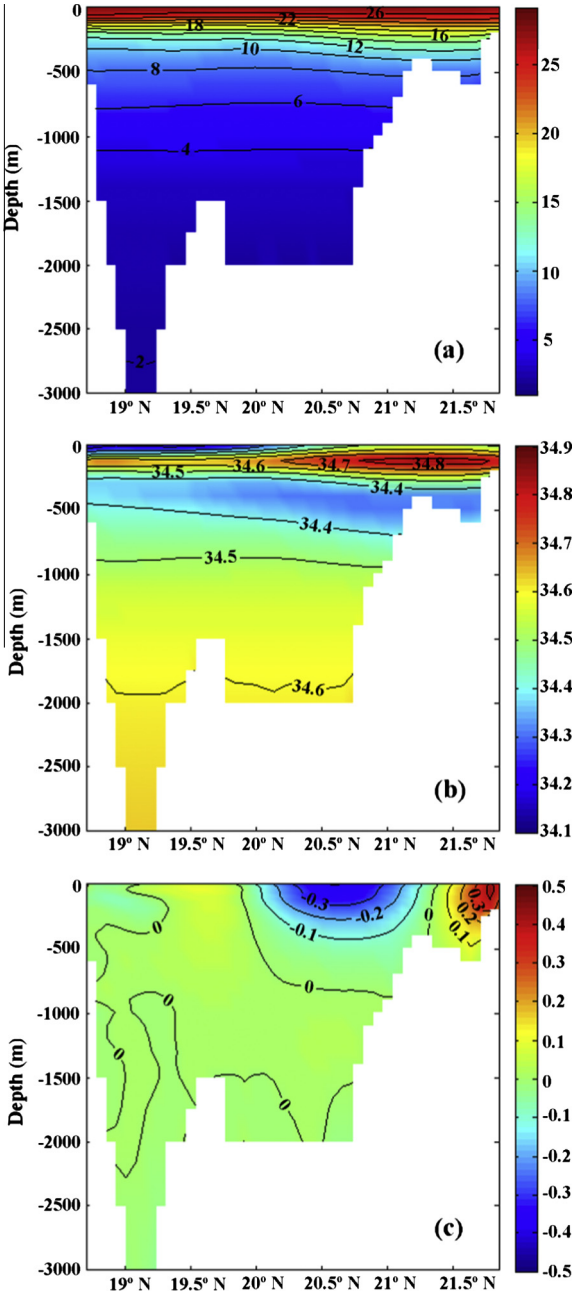

Fig. 5. Annual mean (a) temperature (units: °C), (b) salinity (units: psu), and (c) zonal velocity (units: m s^{-1}) at 120.75°E from 2004 to 2012 based on observation-validated HYCOM output (http://hycom.org/dataserver/glb-analysis).

Fig. 2 in Zhang et al., 2010; Figs. 1, 3 and 4 in Jia and Chassignet, 2011; Nan et al., 2011a), representing one of the best model products to date in describing Kuroshio intrusion into the SCS. From Fig. 5, the flow is dominated by a westward component (inflow) at 20°–21°N and an eastward component (outflow) north of 21°N. The inflow is relatively weak with a maximum speed of about 35 cm/s, but broader than the outflow. The inflow and the outflow form a small anticyclonic bend (see also Fig. 1). The Kuroshio bend varies with time and the looping path occurs when the Kuroshio bend extends westward enough. In the center of the Kuroshio bend, the mean temperature is a little higher than that in the surrounding areas due to downwelling induced by the anticyclonic flow. There exists a salinity maximum (~34.85 psu) at ~150 m depth and a salinity minimum (~34.30 psu) at ~550 m depth (Fig. 5b), representing the North Pacific Subsurface Water and the North Pacific Intermediate Water, respectively. The maximum (minimum) salinity of the Kuroshio water is notably higher (lower) than those of the SCS water (Qu et al., 2000; Li et al., 2002; Zhou et al., 2009). In the center of the Kuroshio bend, the salinity of the subsurface (intermediate) water is saltier (fresher) than that in the surrounding areas. Weak inflows (outflows) are also evident in the deeper layers (below 1000 m), indicating the weak exchange of abyssal water between the SCS and the Pacific. The vertical distribution of the zonal velocity associated with the looping path, the leaking path, and the leaping path can be seen in Fig. 8 of Nan et al. (2011a).

The mean LST was perceived to be a three-layered structure in the vertical from hydrographic data (Chen and Huang, 1996; Qu, 2000; Qu et al., 2006) and lowered ADCP measurements (Tian et al., 2006; Yang et al., 2010), which is westward in the upper and lower layers, and eastward in between. This vertical structure has been widely reproduced by numerical models, though the vertical extension of the outflow varied from model to model. Fig. 6 shows the depth-specific distributions of the mean LST per unit depth at 120.75°E based on the POM (Hsin et al., 2012), HYCOM, and ROMS (Nan et al., 2013). It should be noted that there exists net outflow in the surface layer based on the results of Hsin et al. (2012) and Nan et al. (2013). Satellite-based geostrophic transport in the surface layer is positive due to the net outflow in summer driven by the southwest monsoon, indicating that this layer could be true (Nan et al., 2013). However, it needs to be confirmed by more observational data. Because the northwestern Pacific water is colder and denser, it sinks after crossing the Luzon Strait and contributes to the renewal of the SCS deep water (Wang, 1986; Qu et al., 2004).

Transport of the Kuroshio intrusion into the SCS

It can be seen from Fig. 5 that the Kuroshio intrusion contributes the most to the LST. Though water exchange does occur in the deeper layers, the annual net transport below 750 m is negligibly small (Qu et al., 2004; Nan et al., 2013). The magnitude of the LST often represents the strength of the Kuroshio intrusion in previous studies (*e.g.*, Guo and Fang, 1988; Shaw, 1989; Farris and Wimbush, 1996; Xu and Su, 2000; Zhou et al., 2009). Table 1 summarized results of the LST from long-term observations, short-term cruise data, and numerical models, respectively. Long-term observations were based on dynamical method, P-vector method, diagnostic method, "island rule", Sb-ADCP, and mass balance of historical values, while dynamical method, diagnostic method, and lowered ADCP were used for short-term observations. Based on the long-term observational data, the mean LST was between 3 and 6.5 Sv westward. As mentioned in Section 'Identification of three types of the Kuroshio intrusion into the SCS', the Kuroshio path in the Luzon Strait can change from one path to another in several weeks, this may cause large uncertainties of the observed LST based on short-term cruises. Some snapshot measurements of the LST in summer shows that water flows from the SCS to the Pacific (Yang et al., 2010), which is because the leaping path dominates in the summer (Fig. 7). More long-term consecutive observations are needed in order to reveal the LST variation.

Complementary to the *in situ* observations, a range of numerical models, such as NLOM, POCM, OGCM, MOM2, SODA, MICOM,

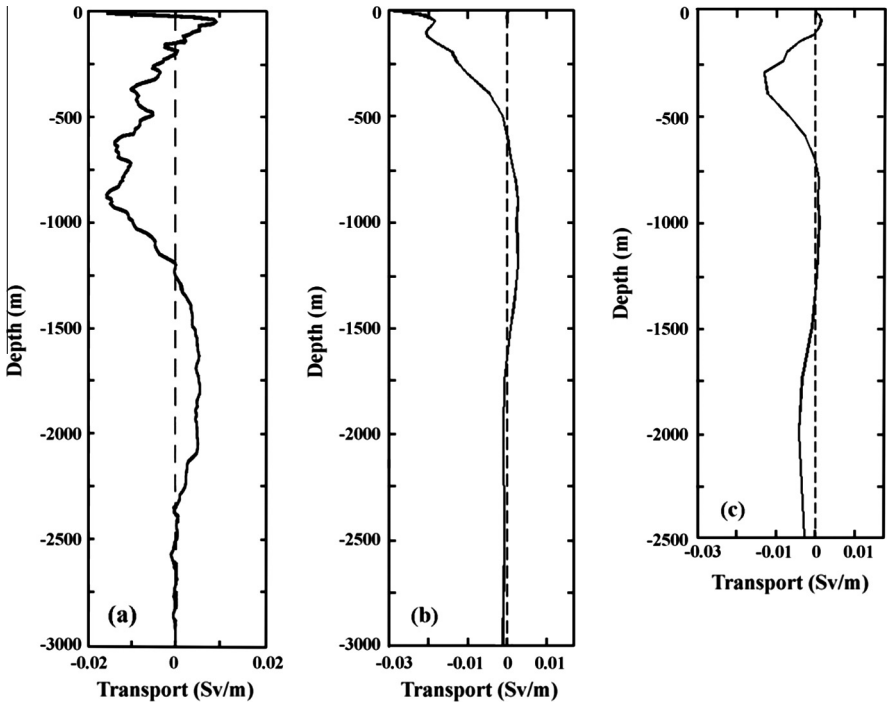

Fig. 6. Depth-specific distributions of mean LST per unit depth (solid line) at 120.75°E based on POM (a) from 2002 to 2008, HYCOM (b) from 2004 to 2012, and ROMS (c) from 1993 to 2012. Figures (a) and (c) were from Hsin et al. (2012) and Nan et al. (2013), respectively, while figure (b) was derived from HYCOM output.

Table 1
Summary of the LST (units: Sv) based on observational data (short-term and long-term) and numerical models. Adapted from Hsin et al. (2012) and some other results were added.

	Transport (depth range in meter)	Method and exploration time
Short-term (<2 months) observations		
Guo and Fang (1988)	−11 to −12 (0–1200)	Dynamic method[a] September, 1995
Xu et al. (2004)	−2.0 (0–1000)	Dynamic method August–September, l994
Xu et al. (2004)	−4.45 (0–1000)	Dynamic method November–December, l998
Tian et al. (2006)	−6 (0–bottom) −9 (0–500) 5 (500–1500) −2 (>1500)	Lowered ADCP[b] October 4–October 6, 2005
Xu et al. (2007)	−6.9 (0–1000)	Dynamic method March 15–March 24, 2001
Liao et al. (2008)	−10.3 (0–400) −7.2 (0–2000)	Dynamic method November 28–December 27, 1998
Yuan et al. (2008a)	−3.5 (0–bottom) −3.5 (0–400) 0.22 (400–1200) −0.22 (1200–bottom)	Diagnostic method[c] August 28–September 10, 1994
Yuan et al. (2008b)	−0.8 (0–400) 2.4 (500–1200)	Diagnostic method March–April, 2002
Yuan et al. (2009)	−3 (0–bottom) −6.6 (0–400) 3.7 (400–2000) −0.1 (2000–bottom)	Diagnostic method March 8–March. 27, 1992
Zhou et al. (2009)	−3.25 (0–1500) −4.47 (0–500) 1.12 (500–1500)	Dynamic method September 18–September 20, 2006
Yang et al. (2010)	5.5 (0–bottom) 5 (0–500) 2.5 (500–1500) −2 (1500–bottom)	Lowered ADCP July 5–July 14, 2007
Yuan et al. (2012)	−4.66 (0–bottom) −2.66 (0–500) 0.74 (500–1200) −2.74 (1200–bottom)	Diagnostic method April 24–June 11, 2008
Yuan et al. (2014)	−2.15 (0–400)	Diagnostic method July 7–July 15, 2009

	Annual	Spring	Summer	Autumn	Winter	Method
Long-term (multi-year) observations						
Wyrtki (1961)	−0.5	0	2.75	−0.5	−2.75	Dynamic method (0–175 m)
Chu and Li (2000)	−6.5			−1.4 (September)	−13.7 (February)	GDEM[d], P-vector[e] method
Qu (2000)	−3.0		−0.2		−5.3	Dynamic method (400 dbar)
Qu et al. (2000)	−4					Island rule[f]
Liang et al. (2003)	−3					Sb-ADCP[g] (0–300 m)
Lan et al. (2004)		−2.5 (April)	−0.29 (July)	−2.44 (October)	−5.53 (January)	GDEM, P-vector method, 0–bottom
Lan et al. (2004)		−1.31 (April)	1.01 (July)	−1.75 (October)	−3.98 (January)	GDEM, P-vector method, 0–500 m
Su (2004)	−4.2 to 5.0					Mass balance of historical values[h]
Yaremchuk and Qu (2004)	−3		−1.2		−4.8	Diagnostic method
Wang et al. (2006c)	−12.4					Island rule
Nan et al. (2013)	−6.9					Island rule
Models						
Metzger and Hurlburt (1996)	−2.4 to −4.4					1/2° global NLOM[i]
Wajsowicz (1999)	−2.85					0.4° global POCM[j] (1987–1995)
Lebedev and Yaremchuk (2000)			−4.7		−6.3	1/6° OGCM[k]
Metzger and Hurlburt (2001b)	−1.8					1/8° north Pacific NLOM
Metzger (2003)	−0.6 to −1.3					1/16° north Pacific NLOM
Fang et al. (2003)	−6.4		−1.16 (June)		−11.27 (January)	1/6° MOM2[l]
Qu et al. (2004)	−2.4		0.9 (June)		−6.1 (January)	1/4° MOM2
Xue et al. (2004)	−2.0					9–12 km regional POM[m]
Fang et al. (2005)	−4.37	−4.78	−1.87	−3.36	−7.47	1/6° MOM2
Song (2006)	−10.2		−8.2		−12.2	1/3–1/2° global model
Wang et al. (2006b)	−1.5					1/2° SODA[n] (1958–2004)
Rong et al. (2007)		−0.74			−3.1	1/2° SODA (1958–2004)
Liang et al. (2008)	−4.8 to −6.5					1/4° MICOM[o] (1996–2001), 0–300 m
Wang et al. (2009)	−4.5		−2.1		−7.6	1/4–2° quasi-global HYCOM[p]
Yaremchuk et al. (2009)	−2.4	−2.1	−0.7	−2.9	−4	1/2° reduced gravity model with data assimilation, 0–700 m
Zhao et al. (2009)	−5.7	−2.6	−1.0	−9.0	−8.1	1/4–2° regional POM
Zhang et al. (2010)	−1.9					1/12° global HYCOM

(*continued on next page*)

Table 1 (*continued*)

	Annual	Spring	Summer	Autumn	Winter	Method
Nan et al. (2011a)	−6.5					1/12° global HYCOM
Hsin et al. (2012)	−4.0 ± 5.1					1/4° regional POM
Nan et al. (2013)	−7.42					1/8° regional ROMS[q]

[a] Geostrophic transport derived from hydrographic data.
[b] Acoustic Doppler Current Profiler.
[c] An extension of dynamic method using hydrostatic balance, continuity, and conservation of potential temperature, salinity, and momentum (Also known as the modified inverse method).
[d] Navy's Global Digital Environmental Model dataset.
[e] Inverse calculation of geostrophic velocity (Chu et al., 1998).
[f] Integrating wind stress over a closed path to derive transport as in Qu et al. (2000) and Wang and Hu, 2006.
[g] Shipboard Acoustic Doppler Current Profiler.
[h] Using the historical transport values of other straits around the SCS to derive the Luzon Strait transport.
[i] Naval Research Laboratory Layered Ocean Model.
[j] Parallel Ocean Climate Model based on the Bryan–Cox model.
[k] Ocean General Circulation Model based on the Bryan–Cox model.
[l] Modular Ocean Model version 2.
[m] Princeton Ocean Model.
[n] Simple Ocean Data Assimilation dataset.
[o] Miami Isopycnic Coordinate Ocean Model.
[p] HYbrid Coordinate Ocean Model.
[q] Regional Ocean Modeling System.

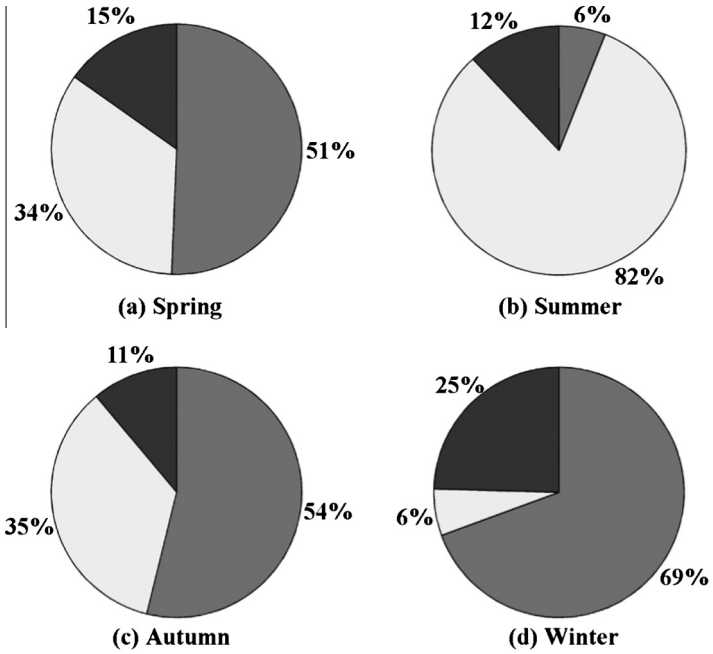

Fig. 7. Seasonal probability of occurrence for the looping path (black), the leaking path (gray), and the leaping path (white) (from Nan, 2012).

HYCOM, POM, ROMS, and reduced gravity model, have been used to simulate the Kuroshio in the Luzon Strait (Table 1). Model estimates of the LST range larger understandably (between 0.6 and 10.2 Sv westward) due to differences in forcing, grid resolution, topography representation, and computation methodology (Hsin et al., 2012). The Kuroshio inflow often appears in the southern side of the Luzon Strait if ignoring the islands in the model setup (Yuan, 2002; Sheremet and Kuehl, 2007; Mu et al., 2011). Metzger and Hurlburt (2001b) indicated that the modeled westward intrusion of the Kuroshio into the SCS weakens with increased horizontal resolution due to improved representation of the bottom topography. Improved three-dimensional models by assimilating available satellite altimeter observations, satellite and *in situ* SST as well as *in situ* vertical temperature and salinity profiles, ARGO floats, and moored buoys should be developed to achieve better comparisons with the observations in future.

Seasonal and interannual variations of the Kuroshio intrusion into the SCS

Spectral analysis of the modeled LST shows that annual and semiannual signals dominate (Hsin et al., 2012). Seasonal and interannual variations of Kuroshio intrusion into the SCS are reviewed in this section. In addition, eddy generation due to change of the Kuroshio paths is also discussed.

Seasonal variation

Kuroshio intrusion into the SCS is seasonally varying. According to historical hydrographic data (Table 1), the LST is larger in winter and smaller in summer in response to the seasonal reversing monsoon (*e.g.*, Wyrtki, 1961; Qu, 2000; Lan et al., 2004; Yaremchuk and Qu, 2004; Xu et al., 2004). There are thousands of satellite-tracked

drifters deployed or drifted into the focused region since 1986, providing direct velocity measurements in the surface mixed layer (Centurioni et al., 2004; Guo et al., 2012). The surface Kuroshio water can intrude deep into the SCS especially in winter derived from Argos satellite-tracked drifters (Centurioni et al., 2004). The water even flows from the SCS to the Pacific in summer according to the results of Wyrtki (1961), Lan et al. (2004), and Yang et al. (2010). Based on water mass analysis, Shaw (1989, 1991) pointed out that Kuroshio intrusion starts in late summer, peaks in winter and ceases by late spring.

Quantitative discrepancies aside, numerical models also reveal a similar seasonality. For examples, Qu et al. (2004) calculated the LST using OGCM model showing that the LST is the largest in winter at about 6.1 Sv (westward), smallest in summer at about −0.9 Sv (eastward). Metzger and Hurlburt (1996) suggested that the westward LST is the largest (8 Sv) in November and smallest (0.5 Sv) in June. Based on the POM model, Hsin et al. (2012) showed that the maximum westward net transport occurs in winter and the minimum in summer. The Kuroshio intrusion is the farthest reaching in December, extending to west of 112°E. In addition, revealed in hydrographic data (Fig. 8 in Shaw, 1991), the Philippine Sea water can be found around 112°E in winter. According to Hsin et al. (2012), the peak-to-peak amplitude of the seasonal cycle for the LST is about 7 Sv. These results imply that the seasonal variation associated with the monsoon is the dominant signal in the LST.

The Kuroshio tends to loop into the SCS more often in winter, while it tends to leap across the LS more often in summer (Wu and Chiang, 2007). Fig. 7 shows seasonal probability of occurrence for the looping path, the leaking path, and the leaping path. It can be seen that the leaking path dominates in winter with the probability of occurrence at 69%, while the leaping path dominates in summer with the probability of occurrence at 82%, i.e., the Kuroshio in winter was likely to penetrate into the SCS and likely to leap across the Luzon Strait in summer. This is the reason why the mean LST is larger in winter and smaller in summer. The looping path appears southwest of Taiwan more frequently in winter than that in other seasons which explains the modeling result of Wu and Chiang (2007). According to Fig. 7, three different Kuroshio paths can occur in any season, which can explain why the short-term observational LST differs considerably in the same season.

Interannual variation

Less is known about the interannual variability of the Kuroshio intrusion into the SCS due to limited available observations (Wu, 2013). The modeling result of Qu et al. (2004) shows that the temporal correspondence of the LST with ENSO is striking, i.e., the LST tends to be higher during El Niño years and lower during La Niña years, with its maximum (minimum) leading the mature phase of El Niño (La Niña) by 1 month. The interannual variation of the LST can be explained by the meridional migration of NEC bifurcation latitude (NBL) (Kim et al. 2004). During El Niño years, the northward shift of the NBL corresponds to a stronger Mindanao Dome and a weaker Kuroshio transport, thus providing a favorable condition for Pacific waters to penetrate into the SCS through the Luzon Strait. The situation is reversed during La Niña years. According to Yaremchuk and Qu (2004), peak-to peak amplitude of the interannual variation is about 3 Sv, smaller than that of the seasonal cycle. The interannual variations of the upper-layer heat content, the SST, and the SSH in the SCS has a strong ENSO signature (Qu et al., 2004; Rong et al., 2007). The linkage between El Niño and the SCS is believed to be through the atmospheric bridge (Wang et al., 2006a). However, on an interannual time scale, the LST from the Pacific into the SCS tends to be higher during El Niño years and lower during La Niña years, and seems to be another key process conveying the ENSO signal from the Pacific into the SCS (Qu et al., 2004; Liu et al., 2008).

As mentioned above, on interannual and longer timescales, most previous studies suggested that the Kuroshio intrusion is generally related to ENSO (e.g., Qiu and Lukas, 1996; Qu et al., 2004; Kim et al. 2004). However, ENSO may not be solely responsible for the atmospheric variability over the northwestern Pacific. A recent study by Wu (2013) showed that the potential impact of the PDO should be taken into account when examining inter-annual variability of currents in the low-latitude northwest Pacific. Especially during the warm PDO phase, an anomalous anticyclonic wind field appeared over the Philippine Sea. The southerly anomalous wind off the Philippines caused a northward shift of the NBL, reducing the Kuroshio transport off Luzon and increasing the Kuroshio intrusion into the SCS. In the cold PDO phase, NBL variations only show a close correspondence with the ENSO. Based on long-term tide gauge and satellite data, Chang and Oey (2012) revealed an interannual oscillation of the ocean's thermoclines east

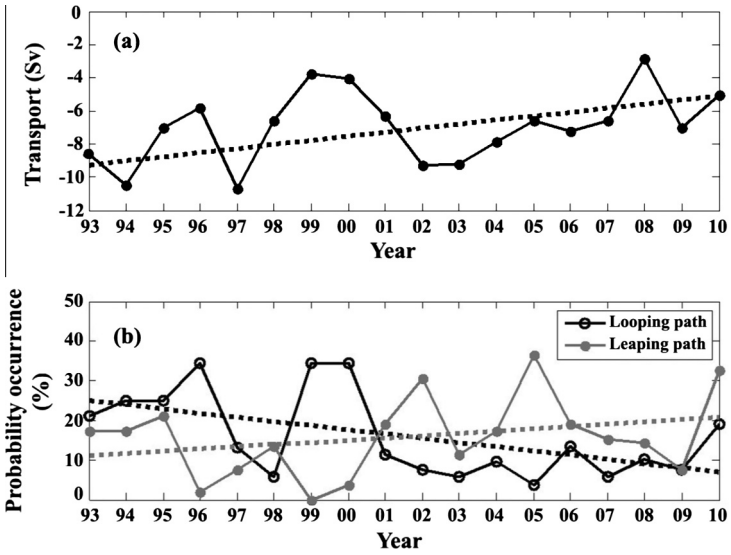

Fig. 8. (a) Yearly time-series and its linear trend of the LST based on ROMS. (b) Yearly time-series and its linear trend of the probability occurrence (units: %) for the Kuroshio intrusion paths near the Luzon Strait. Gray and black lines represent the leaping path and the looping path, respectively. Adapted from Nan et al. (2013).

of the Philippines and Taiwan, forced by a corresponding oscillation in the wind stress curl. It was called Philippines–Taiwan Oscillation (PTO) which was suggested to control the interannual variability of the circulation of the subtropical and tropical northwestern Pacific. In years of positive PTO, the thermocline east of the Philippines rises while east of Taiwan it deepens. This results in a northward shift of the NBL, which increased Kuroshio intrusion into the SCS. The reverse applies in years of negative PTO. The aforementioned indices (ENSO, PDO, and PTO) explain only portions of the interannual variations of the Kuroshio intrusion, since wind, interbasin pressure gradient, β effect and hysteresis, PV, and eddy activity all may contribute to the Kuroshio intruding processes. It will be discussed in detail in Section 'Dynamical mechanisms'.

Based on satellite data, *in situ* hydrographic data, and modeling results, Nan et al. (2013) indicated that the Kuroshio intrusion into the SCS had a weakening trend over the past two decades from 1990s to 2000s (Fig. 8a). The KCL southwest of Taiwan also became weaker. The probability of occurrence for the looping/leaping path has a negative/positive trend (Fig. 8b). Their Pacific ROMS model was forced with the climatological NCEP/NCAR reanalysis of air-sea fluxes for several decades to reach a quasi-equilibrium state. The model was then integrated for the period of 1993–2010 forced with the blended daily sea wind and daily air-sea fluxes of heat and freshwater from the NCEP/NCAR reanalysis. The ROMS modeling result estimated that the Kuroshio intrusion into the SCS became weaker from 1993 to 2010 with a negative trend for the LST at -0.24 Sv yr^{-1}. In response to the weakening Kuroshio intrusion, the mean salinity in the upper water column (from the surface to the intermediate water at ~750 m) decreased in the northern SCS indicating the importance of the Kuroshio intrusion to the heat and salt budgets in the SCS. Although Nan et al. (2013) quantitatively analyzed contributions of the wind, the SSH gradient, and the Kuroshio upstream variation to the LST change, their work is preliminary. The negative trend of the sea-level gradient between the western Pacific and the SCS seems to contribute most of the weakening trend of the Kuroshio intrusion into the SCS.

Eddy generation due to change of the Kuroshio paths

Mesoscale eddies play an important role in the transport of heat, salt, and chemical substances in the SCS (Nan et al., 2011a; Chen et al., 2011a; Wang et al., 2012). Statistical characteristics of eddy activity in the SCS are well documented based on satellite data (*e.g.*, Hwang and Chen, 2000; Wang et al., 2003; Xiu et al., 2010; Chen et al., 2011a; Nan et al., 2011b; Jia and Chassignet, 2011). The results all show that southwest of Taiwan is a region with a high probability of eddy occurrence. Wind stress curl was thought to be an important mechanism of eddy generation in the SCS (Chu et al., 1998; Wang et al., 2007; Pullen et al., 2008; Xiu et al., 2010). However, Nan et al. (2011c) found that the correlation coefficient between the wind stress curl and the eddy occurrence is not significant. They suggested that the Kuroshio path variation is likely the control factor for eddies forming southwest of Taiwan after a comparison of ambient geostrophic currents and eddy occurrence patterns. Based on the statistics of eddy occurrence and the Kuroshio path variation using 17-year satellite altimeter data, Nan et al. (2011c) proposed a conceptual model of eddy-Kuroshio interaction for the summer and winter, respectively (Fig. 9). In summer, the leaping path dominates, i.e., the Kuroshio likely leaps across the Luzon Strait. There exists an outflow northwest of Luzon Island. To the north of the outflow and left of the Kuroshio axis, cyclonic eddies are often formed, which often induce anticyclonic eddies to the west of the cyclonic eddies. In winter, the looping path appears southwest of Taiwan more frequently than other seasons, and anticyclonic eddies are frequently shed from the looping path. As most of the anticyclonic eddies propagate westward, cyclonic eddies are often induced east of the anticyclonic eddies. In this model, variability of the Kuroshio path is emphasized as the control factor for eddies forming southwest of Taiwan, while the direct effect of local wind is less important. However, monsoons are important in driving the SCS outflow in summer and the looping path in winter, both of which have important effects on the seasonal patterns of the eddy occurrence. Responding to the weakened Kuroshio intrusion, the looping path and eddy activity southwest of Taiwan became weaker in 2000s than that in 1990s (Nan et al., 2013). This conceptual model explains why the probability of eddy occurrence is high in the region southwest of Taiwan, providing observational evidence of eddy–Kuroshio and eddy–eddy interactions in the SCS. The shortage of this conceptual model is that it does not cover the situations in spring and autumn.

Dynamical mechanisms

As shown above, Kuroshio intrusion is so important to the momentum, heat and salt budgets, and eddy activity in the SCS that more and more observations and modeling work have been done on the Kuroshio intrusion into the SCS in the past decades. However, the mechanism leading to the Kuroshio intrusion and LST remains controversial to date. To understand what controls the Kuroshio intrusion into the SCS, several factors potentially contributing to the Kuroshio intruding processes, such as wind forcing (local and large-scale), interbasin pressure gradient, β effect and hysteresis, PV, and eddy activity, are reviewed and discussed in this section, respectively.

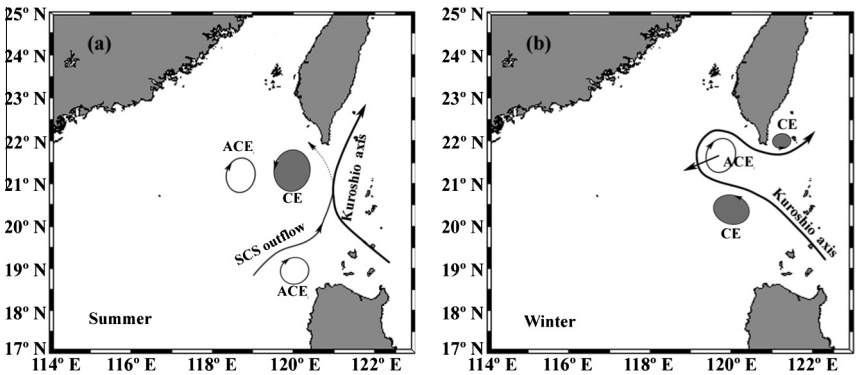

Fig. 9. Schematic showing the Kuroshio paths near the Luzon Strait and formation of cyclonic eddy (CE) and anticyclonic eddy (ACE) southwest of Taiwan (a) in summer and (b) in winter (from Nan et al. 2011c).

Local and large-scale wind forcing

The seasonally reversing monsoon winds in the SCS typically blow from the northeast during boreal winter and from the southwest during boreal summer, and the monsoon is stronger in winter but weaker in summer. Local wind effect plays an important role on seasonal variation of the Kuroshio intrusion into the SCS. There was a close relationship between the mean seasonal cycles of the LST and the northeast-southwest monsoon (Metzger and Hurlburt, 2001a). The first local wind effect is wind-driven Ekman transport, which is negative in the Luzon Strait (from the northwestern Pacific to the SCS) due to northeasterly monsoon in winter and positive (from the SCS to the northwestern Pacific) due to southwesterly monsoon in summer. Negative/positive Ekman transport can enhance/weaken the Kuroshio intrusion, which can contribute to seasonal variation (stronger in winter and weaker in summer) of the Kuroshio intrusion (Wang and Chern, 1987). Wind-induced Ekman transport (calculated using an Ekman depth of ~65 m near the Luzon Strait) is well correlated to the surface geostrophic transport derived from satellite altimeter data through the Luzon Strait (Nan et al., 2011c). However, the purely wind-driven Ekman transport is small, accounting for less than 10% of the total LST (Qu et al., 2004). Besides wind-driven Ekman transport, the local wind can affect the Kuroshio intrusion by changing the Kuroshio inflow angle (Kuehl and Sheremet, 2009) or speed (Hsin et al., 2012) since the Kuroshio inflow direction or speed are important to the Kuroshio path in the Luzon Strait (see Section 'PV conservation'). According to Kuehl and Sheremet (2009), wind-driven Ekman drift can slightly steer the axis of the Kuroshio in the Luzon Strait, which effectively changes the angle of the Kuroshio inflow. Thus the seasonal reversal of the winds may cause seasonal variation of the Kuroshio inflow angle and the LST. Wu and Hsin (2012) and Hsin et al. (2012) conducted a series of experiments using a high-resolution numerical model and suggested that the northeasterly wind in winter intensifies the Kuroshio upstream, enhancing the Kuroshio into the SCS. They also pointed out that without the East Asian monsoon winds the upper-ocean LST changes from westward to eastward. In addition, wind stress curl off southwest Taiwan could be one of the major factors in strengthening Kuroshio intrusions seasonally (Wu et al., 1998). Seasonal occurrence of the three typical paths of the Kuroshio intrusion may also link to the seasonally reversing monsoon winds (Nan et al., 2011c). Farris and Wimbush (1996) have indicated that when a four-day average of the local southward wind-stress component exceeds a critical value, the looping path is initiated.

Besides the local wind forcing, the mean and interannual variability of the LST are affected by the large-scale forcing of the Pacific. For examples, Qu et al. (2005) implied that the variability of the intrusion was primarily forced by large-scale wind forcing over the Pacific Ocean. Wang et al. (2006b) indicates that wind stress in the western and central equatorial Pacific is the key factor regulating the interannual variability of the LST, whereas the effect of local wind stress in the vicinity of the Luzon Strait is secondary. Zhao et al. (2009) also attributed the mean LST to the Pacific basin-scale wind field instead of the SCS monsoon winds. According to Qu et al. (2000) and Wang et al. (2006c), large-scale wind effect can be explained by the "island rule" of Godfrey (1989). Under the steady state and frictionless hypothesis, the LST can be calculated from the line integral of wind stress projected along a closed path ABCD as the following,

$$T_0 = \oint_{ABCD} \tau^{(l)} dl / [\rho_0 (f_D - f_A)]. \quad (2)$$

Here $\tau^{(l)}$ is the wind stress projection along the path ABCD, which can be derived from monthly satellite wind data. A is at the southern tip of Mindanao at 4.75°N, and D is at the northern tip of Luzon at 18.75°N. B and C represent the two points at the same latitudes as A and D at the American coast. The integral taken from D to A is along the western coast of the Philippines. f_A and f_D are the Coriolis parameters at the southernmost (AB) and northernmost (CD) segments of the integral path, respectively. $\rho_0 = 1035$ kg m^{-3} is the mean density of seawater. T_0 calculated from different time-series of wind stress differs greatly in magnitude (Table 1). Yearly variability of the T_0 based on "island rule" has a strong ENSO signal, and is well correlated to the modeling result of Nan et al. (2013). However, long-term change of T_0 is inconsistent with observational and modeling results. It should be noted that the "island rule" is valid for a steady state ocean and ideal fluid only. For a relatively narrow channel like the Luzon Strait, the gap width, bottom topography, friction and other dynamic effects are not negligible (Wang et al., 2006b; Yang et al., 2013b).

In summary, the wind-driven Ekman transport is small compared to the total LST, but local wind can steer the axis of the Kuroshio and change the Kuroshio inflow speed seasonally which effectively contribute to the seasonal variation of the Kuroshio intrusion. Large-scale wind stress in the western and central equatorial Pacific is the key factor regulating the interannual variability of the LST and may convey the impact of the ENSO to the Kuroshio intrusion.

Interbasin pressure gradient

Piling up of water is believed to be an important mechanism by changing the pressure gradient across the Luzon Strait and eventually affecting the Kuroshio intrusion (*e.g.*, Metzger and Hurlburt, 1996; Qu, 2000; Song, 2006). A method to calculate the transport in the straits of Asian marginal seas was proposed by Song (2006). This method combines the "geostrophic control" formula of Garrett and Toulany (1982) and the "hydraulic control" theory of Whitehead et al. (1974), allowing the use of satellite observed SSH and ocean-bottom-pressure data for estimating interbasin transport:

$$Q = \begin{cases} \frac{g}{f} H_1 \Delta\eta + \frac{H_2}{2f} g' \Delta h & \text{if } R < W_0 \\ \frac{g}{f} H_1 \Delta\eta + \kappa \left(\frac{2}{3}\right)^{3/2} H_2 W_0 \sqrt{g' \Delta h} & \text{otherwise} \end{cases}. \quad (3)$$

Here H_1 and H_2 are the surface and bottom layer depth, $\Delta\eta$ is the SSH difference across the sill and Δh is the interface height difference across the sill, g' is the reduced gravity, $R = \sqrt{2g'\Delta h}/f$ is the mean Rossby radius of deformation, $\kappa = sign(\Delta p_b - \Delta\eta)$ determines the gradient direction, and W_0 is the width of the strait. The formulation can be used to separate the surface-layer transport from the bottom-layer transport and to characterize the flow that is governing the water mass in the two adjacent basins.

According to Song (2006), the upper layer (above 1500 m) LST (westward) is controlled by geostrophic balance and can be estimated as $\frac{g}{f} H_1 \Delta\eta$, where $\Delta\eta$ is the SSH difference between the western Pacific (122°E–140°E, 0°N–30°N) and the SCS (105°E–120°E, 0°N–24°N). The estimated LST is larger in winter and smaller in summer and the interannual variation of the estimated LST is closely correlated with the Nino3.4 index in agreement with the observed and modeling results (see Section 'Seasonal variation'). As satellite data are continuous in both space and time, it is convenient to use satellite data in obtaining the LST based on the theory of Song (2006). However, how to choose the western Pacific box is important for the estimation of the interannual variation of the LST. For example, according to Nan et al. (2013), the Kuroshio intrusion into the SCS had a weakening trend over the past two decades in satellite and *in situ* hydrographic data from the 1990s and 2000s. Using the same method, Nan et al. (2013) found that

the interannual variations of the LST is well correlated with $\Delta\eta$, but the long-term change of the LST is opposite to the observed result if the area from 122°E to 140°E and from 0°N to 30°N is chosen as the western Pacific box as in Song (2006). Nan et al. (2013) pointed out that it is more reasonable to select the box (121°E–140°E, 15°–30°N) north of the NEC since the Kuroshio is a part of the subtropical gyre (Fig. 10), for which the long-term change of $\Delta\eta$ agrees with the estimated LST from observations and the model result.

The method proposed by Song (2006) is good to estimate the variation of the LST and does well in explaining the weakening trend over the past decades. However, it should be noted that how to choose the upstream basin (northwestern Pacific) and the downstream basin (the SCS) is very important. On the other hand, the water column was divided into the surface and bottom layers, which excludes the intermediate layer. Thus it cannot reveal the three-layered structure of the LST shown in Section 'Transport of the Kuroshio intrusion into the SCS', which is potentially a drawback of this method.

β effect and hysteresis

The WBC always intrudes as it encounters a meridional gap due to the β effect (Stommel and Arons, 1960). Without the β effect, the LST would be greatly reduced (Yuan, 2002). A number of theoretical works have been devoted to explaining various aspects of gap flow dynamics (Sheremet and Kuehl, 2007; and references therein). According to these theories, there often exist distinct multiple flow patterns for the gap-leaping WBC, which can explain why there are different types of the Kuroshio intruding path.

The transition from one flow state to another for the gap-leaping WBC was investigated by Sheremet (2001). Using a single-layer depth-averaged approach, Sheremet (2001) formulated an idealized model of a western boundary current encountering a gap in a ridge. Multiple flow patterns (penetrating or leaping the gap) exist in such system, which were explained by variations in the balance between the inertia (which promotes the leaping state) and the β effect (which promotes penetrating state). This behavior is analogous to the well-known "teapot effect". Note that the leaping state above corresponds to the leaping path defined in Section 'Identification of three types of the Kuroshio intrusion into the SCS', while the penetrating state corresponds to the leaking path or the looping path since the leaking path and the looping path cannot be separated in the idealized model. Moreover, it was found that a hysteresis exists in transition from one flow state to another: the flow state depends on prior evolution and two different flow states are possible for exactly the same external forcing conditions. Based on this theory, Sheremet (2001) suggested that normally the Kuroshio can leap across the Luzon Strait, whereas it may leak into the SCS during periods when its strength is substantially reduced.

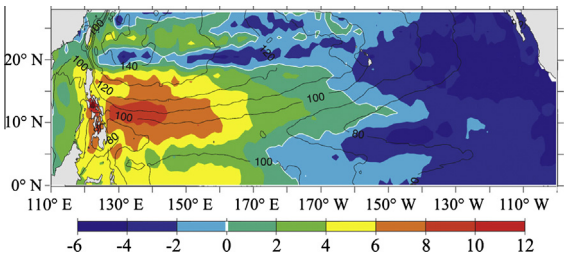

Fig. 10. Linear trend in SSH (mm yr^{-1}) in 1993–2009 derived from the satellite altimeter measurements after removal of the global-mean sea level rise trend of 3.2 mm yr^{-1}. White contours denote the zero linear trend lines, and black contours indicate the mean SSH field (cm) in the Pacific Ocean. Adapted from Qiu and Chen (2012).

The existence of multiple steady states and hysteresis in the gap-leaping problem were confirmed by laboratory experiments of Sheremet and Kuehl (2007) and Kuehl and Sheremet (2009). As shown in Fig. 11, a circular tank with a sloping bottom (mimicking the β effect) is used to set up a gap-leaping current. The gap-leaping current is driven by pumping fluid through sponges (thus generating a Sverdrup flow in the interior). A semicircular ridge with a gap is inserted into the western part of the tank. Using a dye release flow visualization method, change of the flow patterns over varying boundary current transport values are dramatically shown. A series of laboratory experiments were conducted with fixed gap and varied pumping rate Q. The results demonstrated the existence of multiple states (penetrating or leaping the gap) and hysteresis (dependence on past flow state) in the gap-leaping problem (see Fig. 2 in Sheremet and Kuehl, 2007). They also reproduced the laboratory results using a numerical model in bipolar curvilinear coordinates, which allows for the match of the boundaries (Fig. 12). The numerical model predicted two different steady solutions are possible within the range $25 \leqslant Q \leqslant 52(\mathrm{cm}^3\ \mathrm{s}^{-1})$, providing dramatic evidence of multiple steady states and hysteresis. Transitions of multiple steady states were often associated with a cusp catastrophe (small changes in control parameter move the system over the edge and cause large jump in the system state) in the gap-leaping system (Kuehl and Sheremet, 2009), which made the transitions irregular and difficult to predict. The existence of cusp catastrophe in the gap-leaping system can explain why the Kuroshio intruding path can change from one path to another in several weeks. Mesoscale eddies approaching the gap from the eastern basin have significant impact on the WBC path inside the gap (Yuan and Wang, 2011). The effects of mesoscale eddies on the transitions of multiple steady states will be discussed in Section 'Eddy activity'.

It is curious to note that both the laboratory and numerical experiments above are an idealized representation of the WBC encountering a gap in a ridge. It lacks a lot of aspects such as realistic bathymetry, finite curvature of the ridge tip, tilt of the ridge relative to meridian, bottom drag, and stratification. Whether the idealized experiments are suitable to the Kuroshio intrusion into the SCS remains to be evaluated. However, the main similarity is that it can interpret why the Kuroshio in the Luzon Strait exhibits distinct multiple flow patterns. The main implication is that when

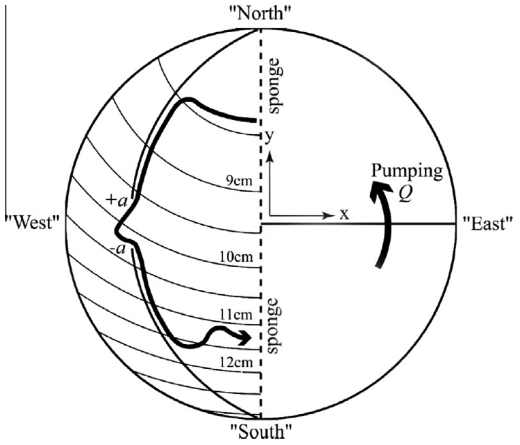

Fig. 11. Sketch of the laboratory experiment for the gap-leaping WBC (from Sheremet and Kuehl, 2007). The barrier is the great circle interrupted by the gap from −a to +a and in the active region the geostrophic contours are shown by thin circular lines. The "western" and "eastern" semicircles are divided by a sponge wall. The eastern semicircle is in turn divided by a solid barrier into the "northern" and "southern" sectors. The flow in the western semicircle is driven by pumping water (with pumping rate Q) from the southern into the northern sectors.

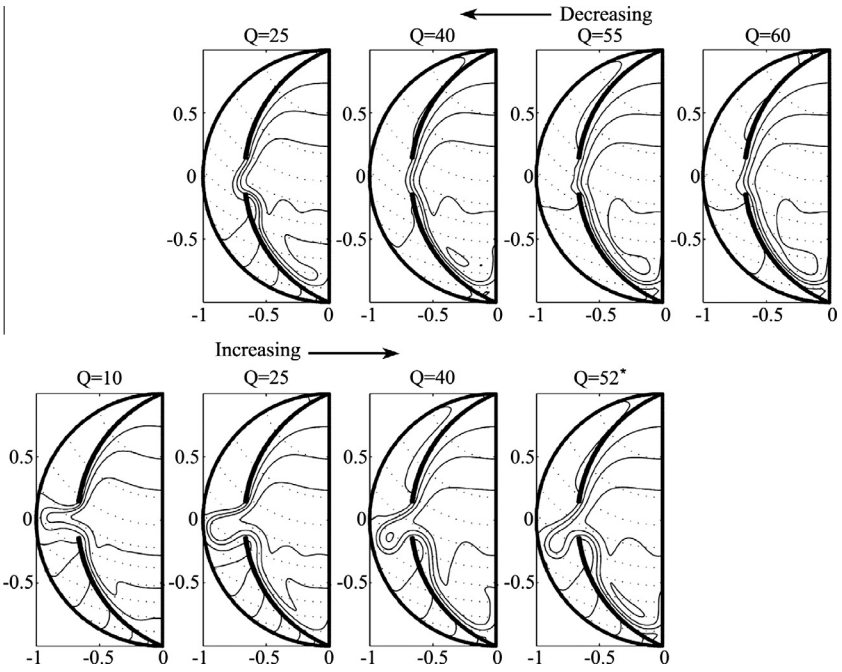

Fig. 12. Steady flow patterns from the numerical solution illustrating the hysteresis as the pumping rate Q is varied (Adapted from Sheremet and Kuehl, 2007). The same parameters as in the laboratory experiments were used in order to reproduce the laboratory results (Fig. 11). The isolines of the total transport are plotted with the contour interval 0.25Q. Shown are two different steady solutions (the leaping state and the penetrating state) by increasing (bottom) and decreasing (top) Q, respectively.

examining the dynamics of the Kuroshio intruding processes, the prior evolution and hysteresis should be taken into account. In addition to β effect and hysteresis, some other factors may also affect transitions between different Kuroshio intruding patterns, such as local wind stress associated with the strong northeast monsoons and the wind stress history (Farris and Wimbush, 1996), and mesoscale flow instabilities caused by eddies arriving from the western Pacific (see Section 'Eddy activity'). Transitions between flow patterns are difficult to predict to date due to the great uncertainty and complexity.

PV conservation

PV distribution across the Luzon Strait plays an important role on the Kuroshio intruding path (Sheu et al., 2010). Assuming PV conservation, Liu et al. (1996) first analyzed the possible paths for the Kuroshio in the Luzon Strait and pointed out that the Kuroshio can intrude into the SCS cyclonically or anticyconically. The Kuroshio in the Luzon Strait satisfies PV conservation was confirmed by Nan et al. (2011a). Analysis of vorticity budget associated with the three Kuroshio intrusion paths shows that in the vorticity equation the baroclinic and frictional contributions are three orders smaller than the tilting of the relative vorticity, stretching of the absolute vorticity, and advection of planetary vorticity, i.e., the Kuroshio in the Luzon Strait satisfies PV conservation (Nan et al., 2011a). How the Kuroshio intrudes into the SCS can be explained dynamically based on PV conservation. Fig. 13 schematically shows of the Kuroshio intruding path west of the Luzon Strait. The equation that describes the Kuroshio intruding path in a simplified β plane, frictionless, steady state, reduced gravity model is given as the following (Xue et al., 2004).

$$\sin\theta\frac{\mathrm{d}\theta}{\mathrm{d}y} = -\frac{\beta}{v_c} + \frac{v_{c0}}{v_c}\sin\theta_0\frac{\mathrm{d}\theta}{\mathrm{d}y}\bigg|_{y=0} \tag{4}$$

where v_c is the speed at the core of the current, and θ is the angle between the velocity vector and the positive x axis as seen in Fig. 13. Derivation of Eq. (4) based on PV conservation can be seen

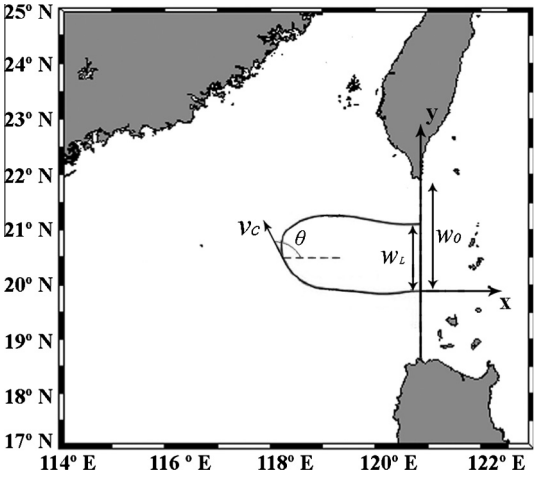

Fig. 13. Schematic of the Kuroshio intruding path west of the Luzon Strait (from Xue et al., 2004).

in (Nan, 2012). If assuming that $v_c = v_{c0}$, $\theta = \theta_0 = \pi$ at the entrance ($y = 0$), Eq. (4) can be integrated and becomes

$$1 + \cos\theta = \frac{\beta}{2v_c}W_L^2 \tag{5}$$

Equation (5) can be easily solved for W_L and the looping path exists only when $W_L < W_0$. However, it can be seen from Figs. 2 and 3 that θ_0 is often not equal to π, and v_c is not constant. In this case, W_L can be obtained from Eq. (6), which depends on the curvature of the streamline at the entrance, the inflow and outflow direction, and the current speed variation (Nan, 2012).

$$\cos\theta = \cos\theta_0 + \frac{\beta}{2v_c}y^2 - y\sin\theta_0\frac{\mathrm{d}\theta}{\mathrm{d}y}\bigg|_{y=0} \tag{6}$$

It can be seen from Eq. (6) that Kuroshio inflow speed and direction are important to the intruding path. As shown in Fig. 2, topography

in the Luzon Strait plays an important role in the Kuroshio intruding position and direction. The Kuroshio flows northwestward into the SCS mainly through the Balintang Channel (~20.5°N) and most of the Kuroshio water flows out of the SCS through the Bashi Channel (*e.g.,* Liang et al. 2003; Liang et al. 2008; Yuan et al. 2008b). If ignoring the islands in the Luzon Strait in the model setup, modeling Kuroshio path will be significantly different (Metzger and Hurlburt, 2001b). On the other hand, changes in the large-scale forcing of the Pacific can lead to the variability in the NEC (Qiu and Chen 2010, 2012) hence the Kuroshio speed and direction east of Philippine. If the upstream Kuroshio changes, the Kuroshio intruding path could respond to it (Qu et al., 2004). Sheu et al. (2010) also pointed that the upstream state of the Kuroshio in the western tropical Pacific plays an important role in determining the different paths of the Kuroshio. From above analysis, we can see that derivation of Eqs. (4)–(6) are based on assumption of steady state, which is unreasonable since the Kuroshio intruding process is unstable (see Section 'Identification of three types of the Kuroshio intrusion into the SCS'). However, Eq. (6) indicates that the Kuroshio intrusion dynamic is a complex nonlinear system.

Eddy activity

Eddy occurrence frequency is high in the Subtropical Countercurrent zonal band between 19°N and 26°N and further elevated near the Luzon–Taiwan coast. Fig. 14 shows the spatial distributions of eddy frequency, mean eddy kinetic energy (EKE), and eddy polarity derived from satellite altimeter data from October 1992 to February 2012. It can be seen that east of the Kuroshio axis in the Luzon Strait is a region with a high probability of eddy occurrence (>30%) and high EKE. According to Yang et al. (2013a), most eddies propagate westward with a mean speed of 7.2 cm s^{-1} and deflect northward following the Kuroshio. Sheu et al. (2010) suggested that westward eddies may propagate freely through the Luzon Strait when the PV across the Kuroshio is weak. However, statistical analysis (Liu et al., 2005; Nan et al., 2011c; Yang et al., 2013a; Lu and Liu, 2013) showed that very few eddies in the northwestern Pacific can enter the SCS due to blocking of the Kuroshio, PV front, and island chain in the Luzon Strait.

Westward eddies may change the Kuroshio speed. Zhao and Luo (2010) investigated the impact of eddies on the Kuroshio in the Luzon Strait using the satellite data and suggested that the Kuroshio can be enhanced (weakened) when a cyclonic (anticyclonic) eddy is far away, whereas it is weakened (enhanced) as the cyclonic (anticyclonic) eddy moves near the Kuroshio. Eddies may also affect the Kuroshio intrusion by changing the Kuroshio inflow direction. Mesoscale eddies generated east of the Luzon Island can cause large oscillations of the Kuroshio axis position from the satellite data (Nan et al., 2013). Local background flow is significantly changed when mesoscale eddies formed or propagated to east of the Luzon Island. The unstable Kuroshio path can be caused by eddies and Rossby waves arriving from the western Pacific (Metzger and Hurlburt, 2001a). Yuan and Wang (2011) conducted a series of numerical experiments on how the gap-leaping WBC change responding to westward eddies. The results shows that transitions of the WBC path from the leaping (leaking) to the leaking (leaping) regimes are induced by cyclonic (anticyclonic) eddies though weakening (enhancing) the inertial advection of vorticity in the vicinity of the gap. The transitions are irreversible because of the nonlinear hysteresis and are found to be sensitive to the strength, size, and approaching path of the eddy. Seasonal variation of eddy activity may affect seasonal fluctuation of the Kuroshio transport east of Taiwan and the LST (Chang and Oey, 2011). However, the yearly EKE in the western Pacific is poorly correlated with the yearly changes of LST (Nan et al., 2013). The effect of eddy activity on the long-term change of the Kuroshio intrusion is not clear now. Quantitative analysis of the eddy activity contributing to change of the Kuroshio intrusion should be conducted in the future.

According to the above discussions, various theories and methods have been used to explain the processes and mechanisms of the Kuroshio intrusion into the SCS. Given the Kuroshio intrusion is a complex nonlinear problem, it is not surprising that different conclusions have been obtained in regarding to the different approaches. This does not necessarily mean that these results conflict with each other, rather, they might refer to explain different phenomenon. As shown in Fig. 15, local and large-scale wind effects play an important role on the seasonal and interannual variations of the Kuroshio intrusion, respectively; interbasin pressure

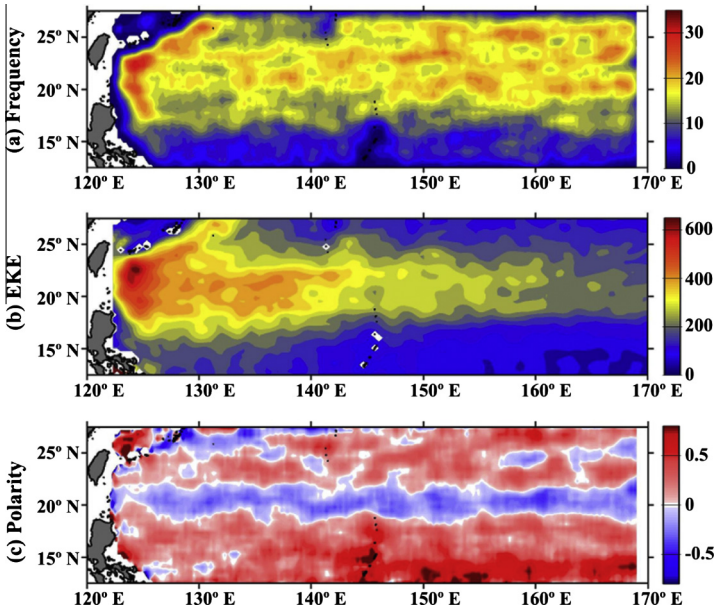

Fig. 14. Spatial distributions of (a) eddy frequency (units: %), (b) mean EKE (units: cm^2 s^{-2}), and (c) eddy polarity (blue for cyclonic eddies and red for anticyclonic eddies) derived from satellite altimeter data from October 1992 to February 2012 (from Yang et al., 2013a).

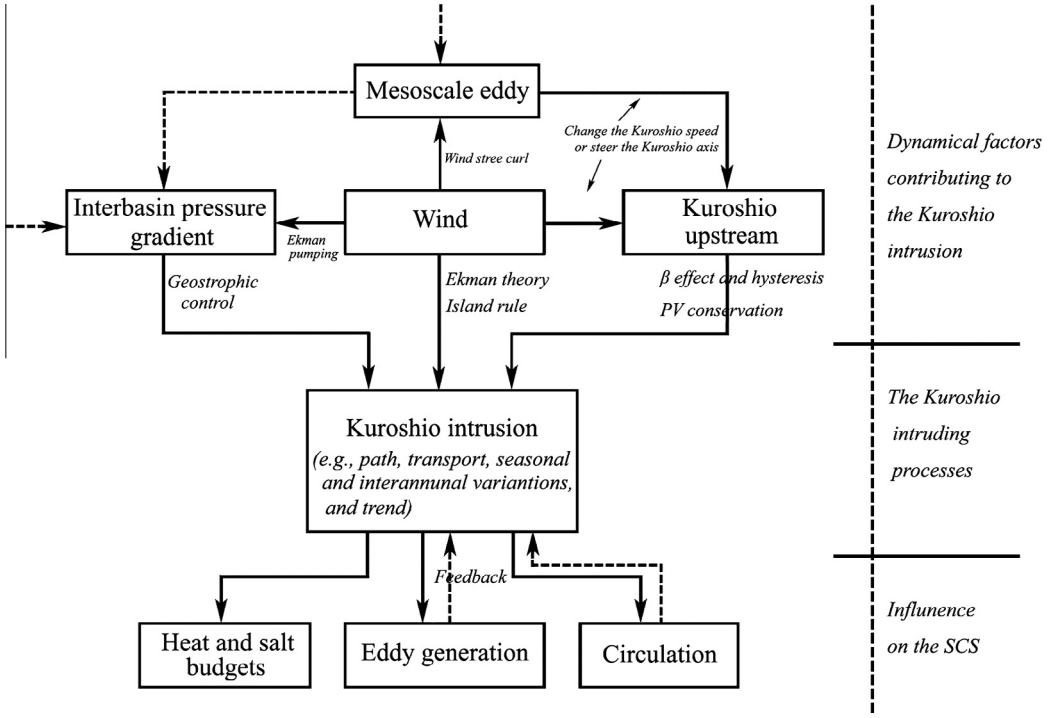

Fig. 15. Schematic of the dynamical factors contributing to the Kuroshio intruding processes and the influence of the Kuroshio intrusion on the SCS. Dotted lines and double question mark denote that the dynamical processes are unclear to date.

gradient change can explain the weakening trend of the Kuroshio intrusion into the SCS; β effect and hysteresis demonstrate why multiple flow patterns exist in such system of the gap-leaping WBC; PV conservation theory shows how the Kuroshio upstream change influences the Kuroshio intruding processes; and westward eddies approaching the gap can change the Kuroshio speed and direction, and then cause the transition of the Kuroshio paths. How the eddy activities and the SCS circulation change affect the Kuroshio intruding processes is unclear. However, to what extent these mechanisms contribute to the Kuroshio intrusion remains to be evaluated.

Summary and future research

The interaction of a boundary current with bathymetric features such as a gap in the ridge or a strait between two islands is an important and interesting oceanographic problem (Stommel and Arons, 1960; Sheremet, 2001; Kuehl and Sheremet, 2009). The Kuroshio between Taiwan Island and Luzon Island is a typical example. In the past decades, the Kuroshio intrusion into the SCS through the Luzon Strait has received increased attention since it is important to the momentum, heat and salt budgets not only in the SCS but also as an integral part of the ITF. In this study, we reviewed past efforts and summarized our current understanding of the Kuroshio intruding processes from observational evidence, laboratory results, theoretical analyses, and a range of numerical model simulations. Note that the Luzon Strait is a primary region for the generation of large amplitude internal solitary waves in the northern SCS, and the Kuroshio intrusion also plays a role on the generation and propagation of internal Guo and Chen (2014) reviewed the observational and modeling results on internal solitary waves induced by the Kuroshio intrusion, which we did not repeat in this study.

In detail, existing studies on Kuroshio intruding paths, vertical structure, transport, seasonal/interannual variations, eddy formation due to the Kuroshio path change, and dynamical mechanisms were reviewed and summarized as follows.

1. On the average, the Kuroshio inflows at 20°–21°N and outflows north of 21°N in the Luzon Strait. The inflow is relatively weak, but broader than the outflow. The Kuroshio inflow and the outflow form the anticyclonic Kuroshio bend. In the center of the Kuroshio bend, the mean temperature is a little higher than that in the surrounding areas due to downwelling induced by the anticyclonic flow. The maximum/minimum salinity of the subsurface/intermediate waters of the Kuroshio water is notably higher (lower) than those of the SCS water. Both observational and model results suggested that the mean LST has a three-layer structure in the vertical: westward in upper and lower depths, and eastward in between. Though water exchange does occur in the deeper layers, the net transport below 750 m is negligibly small, indicating that the Kuroshio intrusion contributes most of the LST. The mean LST derived from multi-year hydrographic data is between 3 and 6.5 Sv westward. Estimates based on short-term cruises, however, are subject to large uncertainties. Model estimates of the LST vary broadly, between 0.6 and 10.2 Sv westward, due to differences in grid resolution, topography representation, and forcing condition.
2. The annual cycle is the dominant signal in the LST with it being larger in winter and smaller in summer, i.e., the Kuroshio intrusion is stronger/weaker in winter/summer confirmed by both observational data and modeling results. On the interannual time scale, the temporal correspondence of the LST with ENSO is striking according to model simulations, i.e., the LST tends to be higher during El Niño years and lower during La Niña years. Kuroshio intrusion seems to be a key process conveying the impact of ENSO from the Pacific into the SCS, which needs to be verified by observational evidence.
3. The Kuroshio intruding path southwest of Taiwan is unstable. The looping path, the leaking path, and the leaping path are

the three typical intruding paths which can be identified quantitatively by geostrophic vorticity southwest of Taiwan (KSI index) and the geostrophic LST based on long-term satellite altimeter data. The Kuroshio path in the Luzon Strait can change from one path to another in several weeks. The leaking path dominates in winter and the looping path appears southwest of Taiwan more frequently in winter than that in other seasons. The leaping path dominates in summer, i.e., the Kuroshio likely leaps across the Luzon Strait in summer.

4. Eddies often form southwest of Taiwan associated with the change of the Kuroshio paths. In summer, the leaping path dominates and often induces cyclonic eddy northwest of the Kuroshio axis. Anticyclonic eddies often exist to the west of the cyclonic eddies. In winter, the looping path appears more frequently southwest of Taiwan. Anticyclonic eddies are often formed and frequently shed from the looping path. As most of the anticyclonic eddies propagate westward, cyclonic eddies are often induced east of the anticyclonic eddies. It is not clear for the dynamics of eddy generation in spring and autumn.
5. The Kuroshio intrusion into the SCS had a weakening trend over the past two decades of 1990s and 2000s inferred from *in situ* observations, satellite data, and modeling results. The probability of occurrence leaping path also has a negative trend, i.e., the Kuroshio is more likely to leap across the Luzon Strait. In response to the weakening Kuroshio intrusion, the mean salinity in the upper water column decreased in the northeastern SCS and eddy activity southwest of Taiwan became weaker in 2000s than that in 1990s.
6. Different mechanisms have been invoked to explain what controls the Kuroshio intrusion into the SCS. In addition to wind forcing, interbasin pressure gradient, β effect and hysteresis, PV conservation, eddy activity, other factors, such as surface heat flux (Hsin et al., 2012), variations inside the SCS (Xue et al., 2004; Wang et al., 2010; Chern et al., 2010), vertical and horizontal mixing, typhoon (Kuo et al., 2011), may also play a role in the Kuroshio intrusion processes.

To sort through the quantitative and conceptual differences, several future research topics on the Kuroshio intruding processes are suggested below.

Observational evidence for interannual and decadal variations

The LST has a negative trend over the past two decades, which has been verified by satellite and *in situ* hydrographic data (Nan et al., 2013). Based on model results, Qu et al. (2004) and Nan et al. (2013) found that the interannual variation of the LST is well correlated to ENSO, i.e., the LST is higher during El Niño years and lower during La Niña years. However, there lack the direct observations supporting the correlation between the LST and ENSO. There are more than 8 thousands of verified temperature-salinity profiles obtained after 1990 in the vicinity of the Luzon Strait (Nan et al., 2013). More and more Argo floats have been deployed in the northwestern Pacific in recent years providing many more temperature-salinity profiles near our study area. These temperature-salinity profiles can be used for examining the interannual and decadal variations of the Kuroshio intrusion based on water mass analysis. The difficulty is how to minimize the bias caused by the temporal and spatial mismatches of temperature-salinity profiles (see Fig. 3 in Nan et al., 2013). In addition, with T–S data, one will need to tease apart the contributions from the surface heat and fresh water fluxes.

Eddy-Kuroshio interaction nearby the Luzon Strait

Eddy occurrence frequency and EKE are high east of the Luzon Strait in the zonal band between 19°N and 26°N (Fig. 14a and b). After generation, most eddies propagate westward but are blocked by the Kuroshio and island chain in the Luzon Strait (Liu et al., 2005; Nan et al., 2011c; Yang et al., 2013a; Lu and Liu, 2013). As shown in Section 'Eddy activity', westward eddies may influence the Kuroshio intrusion by enhancing/weakening the Kuroshio and steering the Kuroshio axis. However, quantitative analysis of the eddy activity contributing to change of the Kuroshio intrusion has not been conducted. On the other hand, it can be seen from Fig. 10 that the SSH increased at a slower rate over the past two decades in the zonal band between 19°N and 22°N compared to other regions of the northwestern Pacific (see also Merrifield and Maltrud, 2011 and Nan et al., 2013). Similarly, cyclonic eddy is predominant in the same zonal band while there are more anticyclonic eddies at most latitudes (Fig. 14c). Conceptually, cyclonic eddy produces upwelling causing negative SSH anomaly. According to Song (2006), long-term change of the SSH east of the Luzon Strait is important to the long-term change of the LST. It is not clear whether the SSH zonal band increased at a slower rate was caused by the predominant westward cyclonic eddies (see Fig. 15). In addition, according to Nan et al. (2011c), southwest of Taiwan is a region with a high probability of eddy occurrence. Eddy activity feedback to the Kuroshio variation has not been studied (see Fig. 15).

Response to the changes of large-scale ocean circulation

Over the past two decades, the subtropical gyre obviously changed. The NEC has a strengthening trend while the NBL was well correlated with the Nino3.4 index and migrated southward over the past two decades (see Fig. 2 in Qiu and Chen, 2012), which can largely be attributed to the upper-ocean water mass redistribution caused by the surface wind stresses of the strengthened atmospheric Walker circulation. Modeling results of Yaremchuk and Qu (2004) indicated that the seasonal variation of LST shows an opposite phase with that of the Kuroshio transport east of Luzon. However, based on a 1/8° Pacific ROMS result, Nan et al. (2013) pointed out that both annual and interannual variations of the Kuroshio transport east of Luzon Island are poorly correlated to those of the LST. To date there is not observational evidence supporting the relationships among the NEC transport, the Kuroshio transport east of Luzon, and the LST. In order to reach a definite conclusion, mooring network and repeated hydrographic surveys in the western Pacific including the NEC, Kuroshio east of Luzon Island, and Kuroshio in the Luzon Strait are needed.

There is no doubt that increasing investigations, including *in situ* measurements, satellite remote sensing, laboratory experiments, theoretical analyses, and numerical simulations, have significantly advanced our knowledge of the Kuroshio intrusion into the SCS and prompt further investigation. However, due to the lack of observations and the complexity of nonlinear dynamics for the Kuroshio intrusion, it still remains unclear what controls the Kuroshio intrusion into the SCS. The investigations appear to be on the right track, but the fundamental mechanism still eludes us and needs to be explored further (Hsin et al., 2012). Essential requirements for better understanding are enhanced observations and improved models. To build a real-time observing system of good accuracy and fine spatial resolution with longterm moorings across the Luzon Strait would be desired in the near future, with the aim to monitor the Kuroshio intruding processes in a comprehensive and systematic way.

Acknowledgements

This work was jointly supported by the National Natural Science Foundation of China (Grant Nos. 41306020 and 91228202), and the National Basic Research Program of China (Grant No. 2010CB950400). We thank all those whose work we have cited as well as those whose reports and publications were not cited, but which have laid the foundation for our knowledge of the region.

References

Caruso, M.J., Gawwarkiewicz, G.G., Beardsley, R.C., 2006. Interannual variability of the Kuroshio intrusion in the South China Sea. Journal of Oceanography 62, 559–575.

Centurioni, L.R., Niiler, P.P., Lee, D.-K., 2004. Observations of Inflow of Philippine Sea Surface Water into the South China Sea through the Luzon Strait. Journal of Physical Oceanography 34, 113–121.

Chang, Y.-L., Oey, L.-Y., 2011. Interannual and seasonal variations of Kuroshio transport east of Taiwan inferred from 29 years of tide-gauge data. Geophysical Research Letters 38, L08603. http://dx.doi.org/10.1029/2011GL047062.

Chang, Y.-L., Oey, L.-Y., 2012. The Philippines–Taiwan oscillation: monsoonlike interannual oscillation of the subtropical-Tropical Western North Pacific wind system and its impact on the ocean. Journal of Climate 25, 1597–1618.

Chen, C.-T., Huang, M.-H., 1996. A mid-depth front separating the South China Sea Water and the Philippine Sea Water. Journal of Oceanography 52, 17–25.

Chen, G.X., Hou, Y.J., Chu, X.Q., Qi, P., 2010. Vertical structure and evolution of the Luzon Warm Eddy. Chinese Journal of Oceanology and Limnology 28 (5), 955–961. http://dx.doi.org/10.1007/s00343-010-9040-3.

Chen, G.X., Hou, Y.J., Chu, X.Q., 2011a. Mesoscale eddies in the South China Sea: mean properties, spatio-temporal variability and impact on thermohaline structure. Journal of Geophysical Research. http://dx.doi.org/10.1029/2010JC006716.

Chen, G.X., Hou, Y.J., Chu, X.Q., 2011b. Water exchange and circulation structure near the Luzon Strait in early summer. Chinese Journal of Oceanology and Limnology 29 (2), 470–481. http://dx.doi.org/10.1007/s00343-011-0198-0.

Chern, C.-S., Wang, J., 1998. A numerical study of the summertime flow around the Luzon Strait. Journal of Oceanography 54, 53–64.

Chern, C.-S., Jan, S., Wang, J., 2010. Numerical study of mean flow patterns in the South China Sea and the Luzon Strait. Ocean Dynamics. http://dx.doi.org/10.1007/s10236-010-0305-3.

Chu, P.C., Chen, Y.C., Lu, S.H., 1998. Wind-Driven South China Sea Deep Sea Basin Warm-Core/Cool-Core Eddies. Journal of Oceanography 54, 347–360.

Chu, P.C., Li, R., 2000. South China Sea isopycnal-surface circulation. Journal of Physical Oceanography 30, 2419–2438. http://dx.doi.org/10.1175/1520-0485(2000) 030<2419:SCSISC>2.0.CO;2.

Dale, W.L., 1956. Wind and drift currents in the South China Sea. The Malayan Journal of Tropical Geography 8, 1–31.

Fang, G.H., Wei, Z.X., Choi, B.H., Wang, K., Fang, Y., Li, W., 2003. Interbasin freshwater, heat and salt transport through the boundaries of the East and South China Seas from a variable-grid global ocean circulation model. Science in China (Series D) 46 (2), 149–161.

Fang, G., Susanto, D., Soesilo, I., Zheng, Q., Qiao, F., Wei, Z., 2005. A note on the South China Sea shallow interocean circulation. Advanced in Atmospheric Sciences 22, 946–954. http://dx.doi.org/10.1007/BF02918693.

Farris, A., Wimbush, M., 1996. Wind-induced Kuroshio intrusion into the South China Sea. Journal of Oceanography 52, 771–784.

Garrett, C.J.R., Toulany, B., 1982. Sea level variability due to meteorological forcing in the northeast of St. Lawrence. Journal of Geophysical Research 87, 1968–1978.

Godfrey, J.S., 1989. A Sverdrup model of the depth-integrated flow for the world ocean allowing for island circulations. Geophysical and Astrophysical Fluid Dynamics 45, 89–112.

Guo, C., Chen, X., 2014. A review of internal solitary wave dynamics in the northern South China Sea. Progress in Oceanography 121, 7–23.

Guo, J.S., Chen, X.Y., Janet, S., Guo, B.H., Qiao, F.L., Yuan, Y.L., 2012. Surface inflow into the South China Sea through the Luzon Strait in winter. Chinese Journal of Oceanology and Limnology 30 (1), 163–168.

Guo, Z.X., Fang, W.D., 1988. The transport of Kuroshio in the Luzon Strait in September 1985. Tropic Oceanography 7 (2), 13–19 (in Chinese with English abstract).

Hu, J., Kawamura, H., Hongi, H., Qi, Y., 2000. A review on the currents in the South China Sea: Seasonal circulation, South China Sea Warm Current and Kuroshio intrusion. Journal of Oceanography 56, 607–624.

Hsin, Y.-C., Wu, C.-R., Chao, S.-Y., 2012. An updated examination of the Luzon Strait transport. Journal of Geophysical Research. http://dx.doi.org/10.1029/2011JC007714.

Hwang, C., Chen, S.-A., 2000. Circulations and eddies over the South China Sea derived from TOPEX/Poseidon altimetry. Journal of Geophysical Research 105 (C10), 23,943–23,965. http://dx.doi.org/10.1029/2000JC900092.

Jia, Y.L., Liu, Q.Y., 2004. Eddy Shedding from the Kuroshio Bend at Luzon Strait. Journal of Oceanography 60, 1063–1069.

Jia, Y.L., Chassignet, E.P., 2011. Seasonal variation of eddy shedding from the Kuroshio intrusion in the Luzon Strait. Journal of Oceanography 67, 601–611.

Kim, Y.Y., Qu, T., Jensen, T., Miyama, T., Mitsudera, H., Kang, H.-W., Ishida, A., 2004. Seasonal and interannual variations of the North Equatorial Current bifurcation in a high-resolution OGCM. Journal of Geophysical Research 109, C03040. http://dx.doi.org/10.1029/2003JC002013.

Kuehl, J.J., Sheremet, V.A., 2009. Identification of a cusp catastrophe in a gap-leaping western boundary current. Journal of Marine Research 67, 25–42.

Kuo, Y.C., Chern, C.-S., Wang, J., Tsai, Y.-L., 2011. Numerical study of upper ocean response to a typhoon moving zonally across the Luzon Strait. Ocean Dynamics 61, 1783–1795. http://dx.doi.org/10.1007/s10236-011-0459-7.

Lan, J., Bao, X., Gao, G., 2004. Optimal estimation of zonal velocity and transport through Luzon Strait using variational data assimilation technique. Chinese Journal of Oceanology and Limnology 22, 335–339. http://dx.doi.org/10.1007/BF02843626.

Lebedev, K.V., Yaremchuk, M.I., 2000. A diagnostic study of the Indonesian Throughflow. Journal of Geophysical Research 105, 11243–11258. http://dx.doi.org/10.1029/2000JC900015.

Li, F.Q., Li, L., Wang, X.Q., Liu, C.L., 2002. Water Masses in the South China Sea and Water Exchange between the Pacific and the South China Sea. Journal of Ocean University of Qingdao 1 (1), 19–24.

Li, L., Wu, B.Y., 1989. A Kuroshio loop in South China Sea?–On circulations of the north-eastern South China Sea. Journal of Oceanography in Taiwan Strait 8 (1), 89–95 (in Chinese with English abstract).

Li, L., Nowlin Jr., W.D., Su, J.L., 1998. Anticyclonic rings from the Kuroshio in the South China Sea. Deep-Sea Research Part I 45, 1469–1482.

Liang, W.D., Tang, T.Y., Yang, Y.J., Ko, M.T., Chuang, W.S., 2003. Upper-ocean currents around Taiwan. Deep-Sea Research II (50), 1085–1105.

Liang, W.D., Yang, Y.J., Tang, T.Y., Chuang, W.S., 2008. Kuroshio in the Luzon Strait. Journal of Geophysical Research 113, C08048. http://dx.doi.org/10.1029/2007JC004609.

Liao, G., Yuan, Y., Xu, X., 2008. Three dimensional diagnostic study of the circulation in the South China Sea during winter 1998. Journal of Oceanography 64, 803–814. http://dx.doi.org/10.1007/s10872-008-0067-4.

Liu, Q.Y., Liu, Z.T., Zheng, S.P., Xu, Q.C., Li, W., 1996. The deformation of Kuroshio in the Luzon Strait and its dynamics. Journal of Ocean University of Qingdao 24 (6), 413–420 (in Chinese with English abstract).

Liu, Q.Y., Daniel, S., Jia, Y.L., Li, W., 2005. Eddies in the northwest subtropical Pacific and their possible effects on the South China Sea. Journal of Ocean University of China 4 (4), 329–333.

Liu, Q.Y., Arata, K., Su, J.L., 2008. Recent progress in studies of the South China Sea circulation. Journal of Oceanography 64, 753–762.

Lu, J., Liu, Q., 2013. Gap-leaping Kuroshio and blocking westward-propagating Rossby wave and eddy in the Luzon Strait. Journal of Geophysical Research: Oceans 118, 1170–1181. http://dx.doi.org/10.1002/jgrc.20116.

Metzger, E.J., Hurlburt, H.E., 1996. Coupled dynamics of the South China Sea, the Sulu Sea, and the Pacific Ocean. Journal of Geophysical Research 101, 12 331–12 352.

Metzger, E.J., Hurlburt, H.E., 2001a. The nondeterministic nature of Kuroshio penetration and eddy shedding in the South China Sea. Journal of Physical Oceanography 31, 1712–1732.

Metzger, E.J., Hurlburt, H.E., 2001b. The importance of high horizontal resolution and accurate coastline geometry in modeling South China Sea inflow. Geophysical Research Letters 28, 1059–1062. http://dx.doi.org/10.1029/2000GL012396.

Metzger, E.J., 2003. Upper ocean sensitivity to wind forcing in the South China Sea. Journal of Oceanography 59, 783–798. http://dx.doi.org/10.1023/B:JOCE.0000009570.41358.c5.

Merrifield, M.A., Maltrud, M.E., 2011. Regional sea level trends due to a Pacific trade wind intensification. Geophysical Research Letters 38, L21605. http://dx.doi.org/10.1029/2011GL049576.

Mu, L., Zhong, L.H., Hua, L.J., Song, J., 2011. Low-frequency variability of a semi-closed sea induced by the circulation in an adjacent ocean in a wind-driven, quasi-geostrophic, eddy-resolving simulation. Ocean Dynamics. http://dx.doi.org/10.1007/s10236-011-0443-2.

Nan, F., Xue, H., Chai, F., Shi, L., Shi, M., Guo, P., 2011a. Identification of different types of Kuroshio intrusion into the South China Sea. Ocean Dynamics. http://dx.doi.org/10.1007/s10236-011-0426-3.

Nan, F., He, Z., Zhou, H., Wang, D., 2011b. Three long-lived anticyclonic eddies in the Northern South China Sea. Journal of Geophysical Research 116, C05002. http://dx.doi.org/10.1029/2010JC006790.

Nan, F., Xue, H., Xiu, P., Chai, F., Shi, M., Guo, P., 2011c. Oceanic eddy formation and propagation southwest of Taiwan. Journal of Geophysical Research 116, C12045. http://dx.doi.org/10.1029/2011JC007386.

Nan, F., 2012. Spatiotemporal Evolution of the Current-Eddy Structure Southwest of Taiwan. Ph.D. thesis, Ocean University of China, 1–119. (in Chinese with English abstract).

Nan, F., Xue, H., Chai, F., Wang, D., Yu, F., Shi, M., Guo, P., 2013. Weakening of the Kuroshio intrusion into the South China Sea over the past two decades. Journal of Climate, doi: http://dx.doi.org/10.1175/JCLI-D-12-00315.1.

Nitani, H., 1972. Beginning of the Kuroshio. In: Stommel, H., Yashida, K. (Eds.), Kuroshio: Physical Aspects of the Japan Current. University of Washington Press, pp. 129–163.

Pullen, J., Doyle, J.D., May, P., Chavanne, C., Flament, P., Arnone, R.A., 2008. Monsoon surges trigger oceanic eddy formation and propagation in the lee of the Philippine Islands. Geophysical Research Letters 35, L07604. http://dx.doi.org/10.1029/2007GL033109.

Qiu, D.Z., Yang, T.H., Guo, Z.X., 1984. A west-flowing current in the northern part of the South China Sea in summer. Tropic Oceanology 3 (4), 65–73 (in Chinese with English abstract).

Qiu, B., Lukas, R., 1996. Seasonal and interannual variability of the North Equatorial Current, the Mindanao Current, and the Kuroshio along the Pacific western boundary. Journal of Geophysical Research 101 (C5), 12,315–12,330. http://dx.doi.org/10.1029/95JC03204.

Qiu, B., Chen, S.M., 2010. Interannual-to-decadal variability in the bifurcation of the north equatorial current off the Philippines. Journal of Physical Oceanography 40, 2525–2538. http://dx.doi.org/10.1175/2010JPO4462.1.

Qiu, B., Chen, S.M., 2012. Multidecadal sea level and gyre circulation variability in the Northwestern Tropical Pacific Ocean. Journal of Physical Oceanography 42, 193–206, doi: http://dx.doi.org/10.1175/JPO-D-11-061.1.

Qu, T.D., 2000. Upper-layer circulation in the South China Sea. Journal of Physical Oceanography 30, 1450–1460.

Qu, T.D., Mitsudera, H., Yamagata, T., 2000. Intrusion of the North Pacific waters into the South China Sea. Journal of Geophysical Research 105 (C3), 6415–6424. http://dx.doi.org/10.1029/1999JC900323.

Qu, T.D., Lukas, R., 2003. The bifurcation of the north equatorial current in the Pacific. Journal of Physical Oceanography 33, 5–18. http://dx.doi.org/10.1175/1520-0485(2003) 033<0005:TBOTNE>2.0.CO;2.

Qu, T.D., Kim, Y.Y., Yaremchuk, M., Tozuka, T., Ishida, A., Yamagata, T., 2004. Can luzon strait transport play a role in conveying the impact of ENSO to the South China Sea? Journal of Climate 17, 3644–3657. http://dx.doi.org/10.1175/1520-0442(2004) 017<3644:CLSTPA>2.0.CO;2.

Qu, T., Du, Y., Meyers, G., Ishida, A., Wang, D., 2005. Connecting the tropical Pacific with Indian Ocean through South China Sea. Geophysical Research Letters 32, L24609. http://dx.doi.org/10.1029/2005GL024698.

Qu, T.D., Girton, J.B., Whitehead, J.A., 2006. Deepwater overflow through Luzon Strait. Journal of Geophysical Research 111, C01002. http://dx.doi.org/10.1029/2005JC003139.

Rong, Z.R., Liu, Y.G., Zong, H.B., Cheng, Y.C., 2007. Interannual sea level variability in the South China Sea and its response to ENSO. Global and Planetary Change 55, 257–272.

Shaw, P.-T., 1989. The intrusion of water masses into the sea southwest of Taiwan. Journal of Geophysical Research 94 (C12), 18213–18226. http://dx.doi.org/10.1029/JC094iC12p18213.

Shaw, P.-T., 1991. The seasonal variation of the intrusion of the Philippine Sea Water into the South China Sea. Journal of Geophysical Research 96 (C1), 821–827. http://dx.doi.org/10.1029/90JC02367.

Sheremet, V.A., 2001. Hysteresis of a western boundary current leaping across a gap. Journal of Physical Oceanography 31, 1247–1259.

Sheremet, V.A., Kuehl, J., 2007. Gap-leaping western boundary current in a circular tank model. Journal of Physical Oceanography 37 (6), 1488–1495.

Sheu, W.-J., Wu, C.-R., Oey, L.-Y., 2010. Blocking and westward passage of eddies in the Luzon Strait. Deep-Sea Research II, doi: 10.1016/j.dsr2.2010.04.004..

Song, Y.T., 2006. Estimation of interbasin transport using ocean bottom pressure: theory and model for Asian marginal seas. Journal of Geophysical Research 111, C11S19. http://dx.doi.org/10.1029/2005JC003189.

Stommel, H., Arons, A.B., 1960. On the abyssal circulation of the world ocean-II. An idealized model of the circulation pattern and amplitude in oceanic basins. Deep-Sea Research 6, 217–218.

Su, F.C., Tseng, R.-S., Ho, C.-R., Lee, Y.-H., Zheng, Q., 2010. Detecting Surface Kuroshio front in the Luzon strait from multichannel satellite data using neural networks. Geoscience and Remote Sensing Letters, IEEE 7 (4), 718–722. http://dx.doi.org/10.1109/LGRS.2010.2046714.

Su, J., 2004. Overview of the South China Sea circulation and its influence on the coastal physical oceanography outside the Pearl River Estuary. Continental Shelf Research 24, 1745–1760. http://dx.doi.org/10.1016/j.csr.2004.06.005.

Tian, J.W., Yang, Q.X., Liang, X.F., Xie, L.L., Hu, D.X., Wang, F., 2006. Observation of Luzon Strait transport. Geophysical Research Letters 33, L19607. http://dx.doi.org/10.1029/2006GL026272.

Wajsowicz, R.C., 1999. Models of the Southeast Asian Seas. Journal of Physical Oceanography 29, 986–1018. http://dx.doi.org/10.1175/1520-0485(1999) 029<0986:MOTSAS>2.0.CO;2.

Wang, J., 1986. Observation of abyssal flows in the northern South China Sea. Acta Oceanographica Taiwanica 16, 36–45 (in Chinese with English abstract).

Wang, J., Chern, C.-S., 1987. The warm-core eddy in the northern South China Sea, I. Preliminary observations on the warm-core eddy. Acta Oceanographica Taiwanica 18, 92–103 (in Chinese with English abstract).

Wang, G., Su, J., Chu, P.C., 2003. Mesoscale eddies in the South China Sea observed with altimeter data. Geophysical Research Letters 30 (21), 2121. http://dx.doi.org/10.1029/2003GL018532.

Wang, Q., Hu, D., 2006. Bifurcation of the North Equatorial Current derived from altimetry in the Pacific Ocean. Journal of Hydrodynamics 18 (5), 620–626. http://dx.doi.org/10.1016/S1001-6058(06)60144-3.

Wang, C., Wang, W., Wang, D., Wang, Q., 2006a. Interannual variability of the South China Sea associated with El Niño. Journal of Geophysical Research 111, C03023. http://dx.doi.org/10.1029/2005JC003333.

Wang, D., Liu, Q., Huang, R.X., Du, Y., Qu, T., 2006b. Interannual variability of the South China Sea throughflow inferred from wind data and an ocean data assimilation product. Geophysical Research Letters 33, L14605. http://dx.doi.org/10.1029/2006GL026316.

Wang, Y., Fang, G., Wei, Z., Qiao, F., Chen, H., 2006c. Interannual variation of the South China Sea circulation and its relation to El Niño, as seen from a variable grid global ocean model. Journal of Geophysical Research 111, C11S14. http://dx.doi.org/10.1029/2005JC003269.

Wang, G., Chen, D., Su, J., 2007. Winter Eddy Genesis in the Eastern South China Sea due to Orographic Wind Jets. Journal of Physical Oceanography 38, 726–732.

Wang, Q., Cui, H., Zhang, S., Hu, D., 2009. Water transports through the four main straits around the South China Sea. Chinese Journal of Oceanology and Limnology 27, 229–236. http://dx.doi.org/10.1007/s00343-009-9142-y.

Wang, G.H., Wang, C.Z., Huang, R.X., 2010. Interdecadal variability of the eastward current in the South China Sea associated with the summer Asian Monsoon. Journal of Climate 23, 6115–6123.

Wang, X., Li, W., Qi, Y., Han, G., 2012. Heat, salt and volume transports by eddies in the vicinity of the Luzon Strait. Deep Sea Research Part I: Oceanographic Research Papers 61, 21–33.

Whitehead, J.A., Leetmaa, A., Knox, R.A., 1974. Rotating hydraulics of strait and sill flows. Geophysical Fluid Dynamics 6, 101–125.

Wu, C.-R., Shaw, P.-T., Chao, S.-Y., 1998. Seasonal and interannual variations in the velocity field of the South China Sea. Journal of Oceanography 54, 361–372.

Wu, C.-R., Chiang, T.-L., 2007. Mesoscale eddies in the northern South China Sea. Deep-Sea Research II 54, 1575–1588.

Wu, C.-R., Hsin, Y.-C., 2012. The forcing mechanism leading to the Kuroshio intrusion into the South China Sea. Journal of Geophysical Research. http://dx.doi.org/10.1029/2012JC007968.

Wu, C.-R., 2013. Interannual modulation of the Pacific Decadal Oscillation (PDO) on the low-latitude western North Pacific. Progress in Oceanography 110, 49–58. http://dx.doi.org/10.1016/j.pocean.2012.12.001.

Wyrtki, K., 1961. Scientific Results of marine investigations of the South China Sea and the Gulf of Thailand 1959–1961. Naga Report, 2, University of California at San Diego, pp. 164–169.

Xiu, P., Chai, F., Shi, L., Xue, H.J., Chao, Y., 2010. A census of eddy activities in the South China Sea during 1993–2007. Journal of Geophysical Research 115, C03012. http://dx.doi.org/10.1029/2009JC005657.

Xu, H.Z., Xu, J.D., Li, L., Chen, J., Du, Y., Wang, D.X., 2007. Hydrography and circulation characteristics about the northeast area of South China Sea during March 2001. Acta Oceanologica Sinica 29 (15), 10–20 (in Chinese with English abstract).

Xu, J.P., Su, J.L., 2000. Hydrological analysis of Kuroshio water intrusion into the South China Sea. Acta Oceanologica Sinica 19 (3), 1–21.

Xu, J.P., Shi, M.C., Zhu, B.K., Liu, Z.H., 2004. Several characteristics of water exchange in the Luzon Strait. Acta Oceanologica Sinica 23 (1), 11–22.

Xue, H.J., Chai, F., Pettigrew, N.R., Xu, D.Y., Shi, M.C., Xu, J.P., 2004. Kuroshio intrusion and the circulation in the South China Sea. Journal of Geophysical Research 109, C02017. http://dx.doi.org/10.1029/2002JC001724.

Yang, Q., Tian, J., Zhao, W., 2010. Observation of Luzon Strait transport in summer 2007. Deep-Sea Research I 57, 670–676. http://dx.doi.org/10.1016/j.dsr.2010.02.004.

Yang, G., Wang, F., Li, Y.L., Lin, P.F., 2013a. Mesoscale eddies in the northwestern subtropical Pacific Ocean: statistical characteristics and three-dimensional structures. Journal of Geophysical Research. http://dx.doi.org/10.1002/jgrc.20164.

Yang, J., Lin, X., Wu, D., 2013b. On the dynamics of the seasonal variation in the South China Sea throughflow transport. Journal of Geophysical Research Oceans 118, 6854–6866. http://dx.doi.org/10.1002/2013JC009367.

Yaremchuk, M., Qu, T., 2004. Seasonal variability of the large-scale currents near the coast of the Philippines. Journal of Physical Oceanography 34, 844–855.

Yaremchuk, M., McCreary Jr., J., Yu, Z., Furue, R., 2009. The South China Sea throughflow retrieved from climatological data. Journal of Physical Oceanography 39, 753–767. http://dx.doi.org/10.1175/2008JPO3955.1.

Yu, X.L., Wang, F., Wan, X.Q., 2013. Index of Kuroshio penetrating the Luzon Strait and its preliminary application. Acta Oceanologica Sinica 32 (1), 1–11. http://dx.doi.org/10.1007/s13131-013-0262-z.

Yuan, D., 2002. A numerical study of the South China Sea deep circulation and its relation to the Luzon Strait transport. Acta Oceanologica Sinica 21 (2), 187–202.

Yuan, D.L., Han, W.Q., Hu, D.X., 2006. Surface Kuroshio path in the Luzon Strait area derived from satellite remote sensing data. Journal of Geophysical Research 111, C11007. http://dx.doi.org/10.1029/2005JC003412.

Yuan, D.L., Wang, Z., 2011. Hysteresis and dynamics of a western boundary current flowing by a gap forced by impingement of Mesoscale Eddies. Journal of Physical Oceanography 41, 878–888, doi: http://dx.doi.org/10.1175/2010JPO4489.1.

Yuan, Y., Liao, G., Guan, W., Wang, H., Lou, R., Chen, H., 2008a. The circulation in the upper and middle layers of the Luzon Strait during spring 2002. Journal of Geophysical Research 113, C06004. http://dx.doi.org/10.1029/2007JC004546.

Yuan, Y., Liao, G., Yang, C., 2008b. The Kuroshio near the Luzon Strait and Circulation in the Northern South China Sea during August and September 1994. Journal of Oceanography 64, 777–788, doi: 10.1007/s10872-008-0065-6.

Yuan, Y., Liao, G., Yang, C., 2009. A diagnostic calculation of the circulation in the upper and middle layers of the Luzon Strait and the northern South China Sea during March 1992. Dynamics of Atmospheres and Oceans 47, 86–113. http://dx.doi.org/10.1016/j.dynatmoce.2008.10.005.

Yuan, Y., Liao, G., Kaneko, A., Yang, C., Zhu, X.-H., Chen, H., Gohda, N., Taniguchi, N., Minamidate, M., 2012. Currents in the Luzon Strait obtained from moored ADCP

observations and a diagnostic calculation of circulation in spring 2008. Dynamics of Atmospheres and Oceans 58, 20–43.
Yuan, Y., Liao, G., Yang, C., Liu, Z., Chen, H., Wang, Z.-G., 2014. Summer Kuroshio Intrusion through the Luzon Strait confirmed from observations and a diagnostic model in summer 2009. Progress in Oceanography 121, 44–59.
Zhai, F., Hu, D., 2013. Revisit the interannual variability of the North Equatorial Current transport with ECMWF ORA-S3. Journal of Geophysical Research 118, 1349–1366. http://dx.doi.org/10.1002/jgrc.20093.
Zhang, Z.G., Zhao, W., Liu, Q., 2010. Sub-seasonal variability of Luzon Strait Transport in a high resolution global model. Acta Oceanologica Sinica 29 (3), 9–17. http://dx.doi.org/10.1007/s13131-010-0032-0.
Zhao, J., Luo, D.H., 2010. Response of the Kuroshio Current to Eddies in the Luzon Strait. Atmospheric and Oceanic Science Letters 3 (3), 160–164.
Zhao, W., Hou, Y.-J., Qi, P., Le, K.-T., Li, M.-K., 2009. The effects of monsoons and connectivity of South China Sea on the seasonal variations of water exchange in the Luzon Strait. Journal of Hydrodynamics 21, 263–270. http://dx.doi.org/10.1016/S1001-6058(08)60144-4.
Zhou, H., Nan, F., Shi, M.C., Zhou, L.M., Guo, P.F., 2009. Characteristics of water exchange in the Luzon Strait during September 2006. Chinese Journal of Oceanology and Limnology 27 (3), 650–657. http://dx.doi.org/10.1007/s00343-009-9175-2.